THESIS

HYDROTHERMAL MINERALIZATION AND ALTERATION AT THE GLOBE HILL DEPOSIT, CRIPPLE CREEK DISTRICT, COLORADO

Submitted by

Alan D. Trippel

Department of Earth Resources

In partial fulfillment of the requirements

for the Degree of Master of Science

Colorado State University

Fall 1985

COLORADO STATE UNIVERSITY

May 10, 1985

WE HEREBY RECOMMEND THAT THE THESIS PREPARED UNDER OUR SUPERVISION BY ALAN D. TRIPPEL ENTITLED HYDROTHERMAL MINERALIZATION AND ALTERATION AT THE GLOBE HILL DEPOSIT, CRIPPLE CREEK DISTRICT, COLORADO BE ACCEPTED AS FULFILLING IN PART REQUIREMENTS FOR THE DEGREE OF MASTER OF SCIENCE.

Committee on Graduate Work

Stan W. Caddey

Tommy B. Thompson
Adviser

Department Head

ABSTRACT

HYDROTHERMAL MINERALIZATION AND ALTERATION AT
THE GLOBE HILL DEPOSIT, CRIPPLE CREEK DISTRICT, COLORADO

The Globe Hill deposit is hosted by a porphyritic, subvolcanic intrusive which is composed of pyroxene-bearing alkali trachyte. It is emplaced within the Oligocene-age Cripple Creek diatreme-intrusive complex, which may be related to the Rio Grande rift system centered 75 km to the west.

Four structural events occurred at Globe Hill. The earliest event (stage I) created a zone of upward-flaring hydrothermal breccia bodies which were later cut by a series of tectonic structures (stage II). A dike- or column-like body of intrusive breccia (stage III) subsequently invaded a major stage II shear zone, and a large, separate hydrothermal breccia body (stage IV) formed within the stage I zone.

Separate hydrothermal fluids passed through each of the structural systems, and formed epithermal, low-grade, polymetallic mineralization along stage I, II, and IV structures; stage III structures remained unmineralized. Mineralization occurs as veins, breccia-matrix fillings, and disseminations through breccia fragments and adjacent wall

rock. Stage I structures were mineralized by an assemblage composed dominantly of chalcedony-celestite-pyrite and trace oxides, telluride, phosphates, and base-metal sulfides. Early stage II veins are composed dominantly of quartz-celestite-pyrite and trace adularia, oxides, telluride, and base-metal sulfides. Wallrock adjacent to later stage II gangue-free structures contains halos of disseminated pyrite and trace oxides, telluride, and base-metal sulfides. The central core zone of the stage IV breccia is cemented by an assemblage of anhydrite-carbonate-celestite-fluorite along with trace pyrite, oxides, and base-metal sulfides; its peripheral halo is partially cemented by montmorillonite and minor amounts of fluorite, quartz, and hematite.

Five separate alteration events are recognized. Each of the first four is hypogene and correspond to one of the major structural stages. The fifth event is related to supergene weathering. Alteration associated with the stage I hydrothermal breccias grades from a sericite-dominated zone within the breccia bodies to a chlorite-dominated zone in the surrounding wallrock. Wallrock adjacent to stage II tectonic structures has been altered to a sericite-dominated assemblage. Alteration of the stage III intrusive breccia primarily affected the matrix material and to a lesser extent the fragments, producing a chlorite-dominated assemblage. Stage IV central core zone breccia fragments were altered to a quartz-dominated assemblage which grades to a montmorillonite-dominated assemblage in the peripheral zone and wallrock. The last hypogene event as well as the supergene weathering have partially oxidized the deposit to a depth of over 270 m. The effects of supergene weathering are most pronounced along stage I and II structures where permeability is sufficient to allow for downward percolation of oxidizing surface waters.

Mineralization and alteration assemblages associated with each structural stage have been used to infer parent-fluid chemistry. Existing data suggest that the fluids were weakly to moderately alkaline, moderately oxidized, and of relatively low sulfur fugacity. Certain fluids associated with stage I, II, and IV structural stages must have contained appreciable amounts of Ca, Sr, phosphate, sulfate, and dissolved gases including CO_2 and H_2S. Zonal wallrock alteration assemblages indicate intermediate to weak metasomatic reactions adjacent to each structure.

Boiling is interpreted as the major cause of mineral precipitation along stage I, early stage II, and stage IV structures. Evidence for boiling fluids includes the development of hydrothermal breccias, often along veins; explosion textures in vein quartz and celestite; the occurrence of adularia in some vein assemblages; and the highly variable vein fluid-inclusion homogenization temperatures and liquid to vapor ratios. The relatively restricted extent of most alteration zones suggests that groundwater mixing and metasomatic wallrock interactions occurred. These two processes could rapidly promote fluid-groundwater and fluid-wallrock equilibration, terminating further alteration. No evidence for fluid boiling was observed along the later stage II tectonic structures; in this case, metasomatic wallrock interactions were the major cause of mineral precipitation.

The Globe Hill gold deposit may be the near-surface (hot-springs) expression of deeper, high-grade vein deposits like those located elsewhere in the district. Mineralizing fluids probably were convectively circulated by a thermal anomaly at depth beneath the Globe Hill area. The thermal anomaly and the presence of appreciable Ca and Sr in the fluids were probably derived from late alkali basalt igneous activity within the Cripple Creek diatreme-intrusive complex.

Alan D. Trippel
Department of Earth Resources
Colorado State University
Fort Collins, Colorado 80523
Fall, 1985

ACKNOWLEDGEMENTS

The author gratefully acknowledges the cooperation and financial support provided by Brian Hester and Peter Reed at Gold Resources, Inc., Ken Ennis at Newport Minerals, Inc., and Steve Peters at Texasgulf Metals Co. Sincere thanks is extended to Drs. Tommy Thompson (CSU), Stan Caddey (Homestake Mining Co.), and John Vaughan (CSU) for their invaluable constructive criticism of the project; to Dr. Jay Gregg and David Brosnahan (St. Joe Minerals Corp.) for providing EDS analyses; to Denny Heyrman and Jack Rogers (CSU) for field assistance; and to Rick Trippel (Consulting Geologist) for drafting.

Standard Oil Co. of California (Chevron) provided financial assistance through a generous field-oriented thesis grant. The cost of supplying and maintaining fluid-inclusion analysis equipment was supported by the Economic Geology Development Fund at Colorado State University.

I have the greatest appreciation for my wife, Vicki Fulkerson, who provided her geologic assistance and excellent technical editing skills and who possessed tireless patience throughout the entire project.

TABLE OF CONTENTS

Page

LIST OF FIGURES

Fig. 12. Stage IV hydrothermal breccia of the central core zone, with anhydrite matrix-filling (gray) partially weathered to gypsum (white). Note dark-colored silicified fragment (arrow).

Fig. 13. Thin-section photomicrograph (plane light) of explosion texture in euhedral quartz of a stage I vein. Quartz margin intergrown with fluorite; matrix mostly fluorite. Field of view is 1.8 mm wide.

Fig. 14. Back-scattered electron image from a polished-section of stage I replacement mineralization in a breccia fragment. Sample shows monazite (1: white, subhedral, prismatic crystals), pyrite (2: gray-white, rectangular crystals), and anatase (3: gray, irregular aggregates) in altered wallrock (dark gray and black). Pyrite is partially replaced by anatase. Field of view is 0.62 mm wide.

Fig. 15. Generalized paragenetic diagram of mineralization associated with each structural stage at the Globe Hill deposit. Width of lines show relative abundances; dashed line indicates sporadic deposition.

Fig. 16. Quartz vein along early-formed stage II tectonic structure. Narrow white band along vein margin is a zone of explosion texture which contains sulfides, oxides, and telluride coprecipitated with quartz. Yellow stain on wallrock due to sodium cobaltinitrite.

Fig. 17. Thin-section photomicrograph (X-nicols) of a quartz vein along an early-formed stage II tectonic structure. Fracture in wallrock (dark aggregate) is rimmed by adularia (dark gray rhombs), and filled with quartz (white and light gray). Field of view is 0.6 mm wide.

Fig. 18. Thin-section photomicrograph (X-nicols) of fan-like aggregates of bladed anhydrite in stage IV central core zone breccia matrix. Note the curved cleavage planes and crystal faces, and the planes of abundant fluid inclusions (dark specks). Field of view is 0.25 mm wide.

Fig. 19. Thin-section photomicrograph (X-nicols) of stage I chlorite (fine-grained green-gold)-sericite (coarser, brilliant blades)-pyrite (opaque) alteration of wallrock (gray phenocrysts and groundmass) which surrounds the hydrothermal breccia bodies. Field of view is 1.8 mm wide.

Fig. 20. Thin-section photomicrograph (X-nicols) of sericite (fine-grained, brilliant)-montmorillonite-carbonate-pyrite (opaque) alteration of wallrock (gray) adjacent to gangue-free stage II tectonic structures. Field of view is 2.0 mm wide.

LIST OF TABLES

LIST OF PLATES

CHAPTER 1

INTRODUCTION

The Cripple Creek mining district is located in Teller County, Colorado, 30 km west of Colorado Springs and 9 km southwest of Pikes Peak (Fig. 1). Since its discovery in 1891, the district has produced almost 21 million troy ounces of gold (Gott et al., 1967) and over 2 million troy ounces of silver (Koschmann, 1960), most of which has been from high-grade vein deposits near the margin of the district.

Production peaked in 1900 when 879,000 troy ounces of gold were processed from Cripple Creek ores. By 1920, production had drastically decreased due to labor shortages, wage disputes, and water problems, but surprisingly not to decreased grades or tonnages of ore. Mining was revitalized in 1933, when the price of gold rose from $20.67 to $35.00 per troy ounce, and continued moderately until 1942, when government regulations and wartime restrictions all but halted gold production. With the lifting of price restrictions on gold in the early 1970's, renewed interest in the district focused on bulk-tonnage deposits amenable to low-cost, open-pit mining methods such as is found at Globe Hill (Fig. 2).

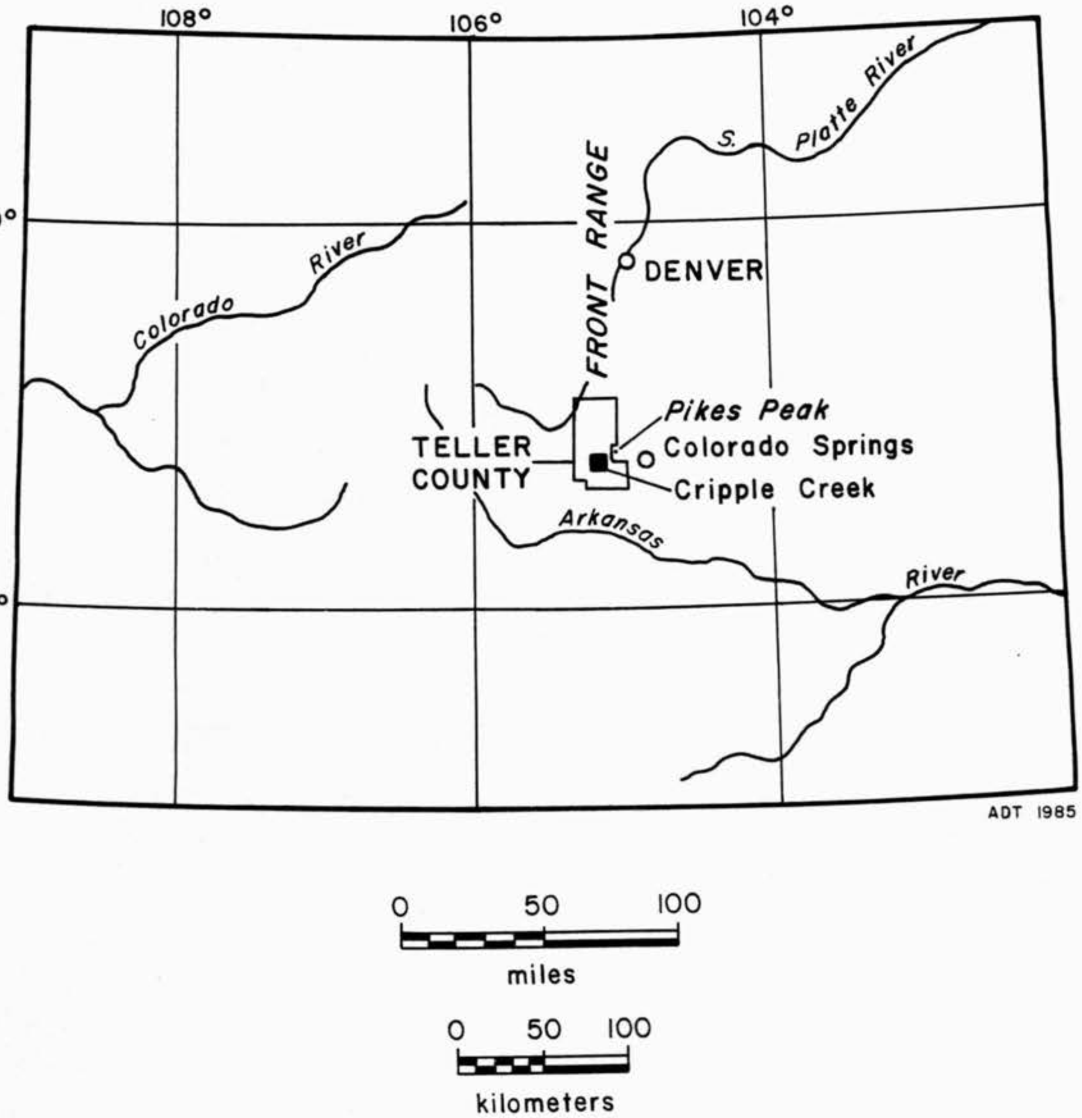

Fig. 1. Location of the Cripple Creek district, Colorado.

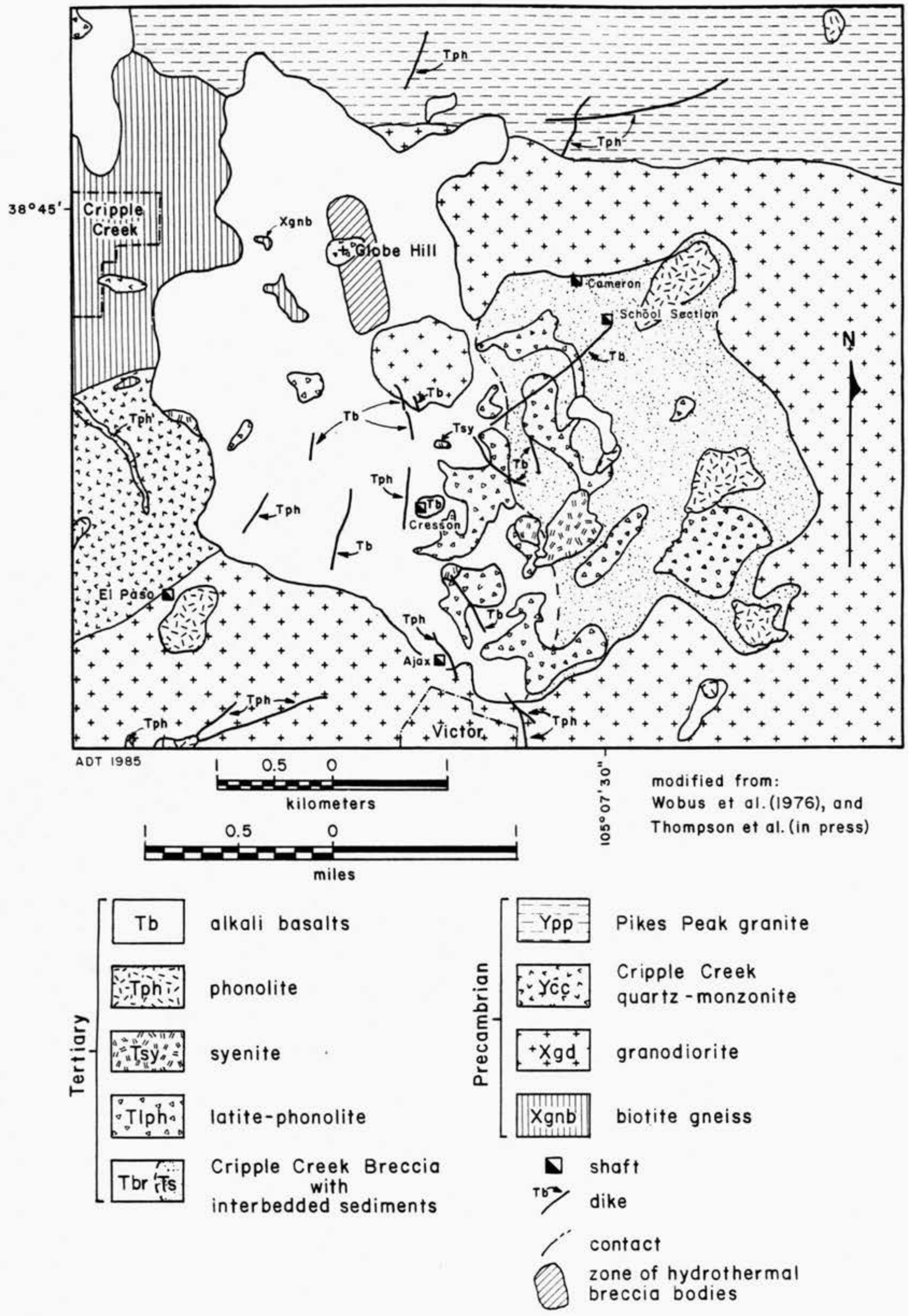

Fig. 2. Geologic map of the Cripple Creek diatreme-intrusive complex.

The geology of the Cripple Creek district is described in many published reports, beginning with Cross and Penrose (1895). Soon afterward, Lindgren and Ransome (1906) completed the most valuable publication on the district; it contains detailed descriptions of rock types, structures, and mineralization at numerous mines, nearly all of which are inaccessible today. Other important works, including Loughlin and Koschmann (1935), Koschmann (1941, 1949), Keener (1962), and the unpublished field maps compiled by Koschmann and Loughlin (1965), have contributed significantly to recent models on the formation of the district. The most recent data and modern interpretations are presented by Wobus, Epis, and Scott (1976), Sillitoe and Bonham (1984), and Thompson, Trippel, and Dwelley (in press).

Gold production from the summit of Globe Hill (elev 3183 m) began in 1891 when land claimed by Matt Sterret was mined for its high-grade gold in quartz-vein float with the aid of a plow (Sprague, 1953). At least 80,000 troy ounces of gold were subsequently recovered from the high-grade gold veins and fault structures of the Deerhorn, Summit, and Plymouth Rock No. 1 mines (Plate 1) and from the short Globe Tunnel which intersected the upper level of the Deerhorn mine.

Between 1899 and 1902, the Chicago and Cripple Creek Tunnel (elev 2957 m) was extended in order to explore the vein potential at depth beneath Globe Hill. The tunnel is about 1280 m long and extends from Poverty Gulch eastward to intersect the Plymouth Rock No. 1 shaft (Plate 1). Although no high-grade ore was discovered, highly altered and oxidized breccia containing trace and low-grade gold was noted over a considerable distance (Argall, 1905).

By 1905 two small open pits (Globe, Deerhorn) were excavated to a depth of 15 m along intersecting veins and fault structures exposed at the surface near the summit of Globe Hill.

From 1916 to the mid-1970's there was little production from the area. However, numerous exploration programs were conducted to evaluate the low-grade (0.0X troy oz/t Au) surface mineralization by means of bulk sampling, trenching, and drilling.

From 1977 to 1981 Newport Minerals, Inc., a subsidiary of Gold Resources, Inc., mined 680,000 tons of low-grade gold ore from the Globe Hill pit, centered on the old Globe and Deerhorn pits (Plate 1). Mining was halted in 1981 to allow Texasgulf, Inc., a joint-venture partner at that time, to conduct a detailed evaluation and feasibility study of the deposit. The evaluation included drilling, trenching, sampling, and mapping. Production is expected to resume in 1985.

Since March, 1981, Silver State Mining Corp. has operated a 1000-ton-per-day open-pit mine located at the old Ironclad pit, half a kilometer southeast of Globe Hill (Lewis, 1982; Plate 1). In mid-1984, Nerco Minerals Co. entered a joint-venture agreement with Silver State and has since become the operator of the mine. The geology and gold mineralization is poorly understood, but brief visits by the author indicate many similarities to, and perhaps extensions of, features exposed in the Globe Hill pit.

Numerous publications and reports discuss the Globe Hill area. They include Cross and Penrose (1895), Argall (1905, 1908), Lindgren and Ransome (1906), Keener (1962), and Peters (1982). None, however, fully describe and interrelate the structure, mineralization, and alteration. Therefore, the primary objective of this study is to document the bulk-tonnage deposit at Globe Hill, including the host lithology, structure, mineralization, alteration, and geochemistry. This information will then be incorporated into a model explaining the processes responsible for the mineral deposit.

Toward this goal, the Globe Hill pit was mapped at 1:240 scale, 1005 m of available core from Globe Hill were logged at 1:120 scale, and approximately 3 square kilometers of the district geology surrounding Globe Hill were mapped at 1:6000 scale. Field work was conducted for eight weeks during the summer and fall of 1983.

Rock samples collected during the field season were examined during the fall of 1983 and winter of 1984 by means of the following laboratory techniques: preparation and microscopic examination of 75 petrographic thin sections and 45 polished sections; preparation of, and fluid inclusion heating studies on, 15 doubly-polished plates; and preparation and X-ray diffraction analysis of select mineral phases. Additionally, 53 rock chip samples were analyzed geochemically for 13 elements.

CHAPTER 2

REGIONAL GEOLOGY

The Cripple Creek breccia-alkaline-intrusive complex, major host of the mineralization which formed the ore deposits of the Cripple Creek district, was developed during the Oligocene epoch at the intersecting contacts of four widespread Precambrian lithologic units (Fig. 2). The oldest of these units extends to the west of the Cripple Creek complex and is described by Wobus et al. (1976) as a layered biotite-quartz-plagioclase gneiss which is locally sillimantic or migmatitic. Barker et al. (1975) believe this biotite gneiss to be the amphibolite-grade metamorphic equivalent of 4500 vertical meters of widespread basaltic and acidic volcanics and pelitic sediments deposited 1700 to 1400 million years ago (mya), or during Precambrian X time. A Rb/Sr date on this gneiss is reported as 1690 mya (Hutchinson and Hedge, 1968).

The next youngest and most widespread of the four units is described by Wobus et al. (1976) as a foliated hornblende- or biotite-granodiorite of Precambrian X age. This granodiorite occurs as blocks and partially-exposed ridges within the complex, and extends outward more than 10 km to the southwest, south, and east.

Relatively soon afterward, the Cripple Creek quartz-monzonite was emplaced. This two-mica, intrusive rock is found to the west, outside the complex margin (Wobus et al., 1976). It is dated at 1430 mya (Rb/Sr; Hutchinson and Hedge, 1968), or Precambrian Y, and is a part of the Silver Plume igneous event which occurred throughout the southern Rocky Mountains (Barker et al., 1975).

The Pikes Peak granite, dated at 1040 mya, or Precambrian Y (Barker et al., 1975), is the youngest of the four units and is described by Wobus et al. (1976) as a biotite to hornblende-biotite granite and quartz-monzonite. This unit extends to the north of the complex and forms the southernmost portion of the Pikes Peak batholith. The batholith is described by Barker et al. (1975) as being anorogenic, intracratonic, and composed of sodic to potassic intrusions which were emplaced to a shallow crustal level; it is probably underlain by a layered gabbroic-anorthositic body.

Much of central Colorado, including the entire Cripple Creek area, is completely void of Palezoic and Mesozoic sedimentary rocks. These rocks are presumed by Chapin and Epis (1964) to have once been a thick, widespread sequence which was completely eroded in central Colorado prior to Tertiary igneous activity.

The Laramide compressional event occurred between 70 to 55 mya, or late Cretaceous to early Eocene, in the southern Rocky Mountain region (Tweto, 1975). Its effects on the

Cripple Creek area include broad doming of the Precambrian rocks and formation of major fractures both oblique and transverse to the dome (Loughlin and Koschmann, 1935). Intersecting fracture sets may have been a critical factor in localization of the Cripple Creek complex.

The Laramide event was followed by igneous activity which produced thick, widespread, intermediate-composition volcanic ash-flow units covering much of the southern Rocky Mountain region. Steven (1975) believes that the volcanism originated from several separate centers, the largest of which created the San Juan volcanic field, between 40 and 25 mya. Lipman et al. (1972) attribute the Laramide compression and this later intermediate-composition volcanic activity to an eastward-dipping slab of a large, imbricate subduction zone west of Colorado. They place the slab as dipping beneath the eastern Colorado Plateau and the southern Rocky Mountains.

The Thirty-nine Mile field, centered 15 to 18 km west of Cripple Creek, and dated at 35 to 30 mya (Steven, 1975), is another of these intermediate-composition volcanic fields. Portions of its units are exposed 5 km southwest of the Cripple Creek complex (Wobus et al., 1976). Chapin and Epis (1964) noted that, while much of the section is andesite, the middle layers contain thick ash-flows of rhyolite (with a high volatile content) and pyroxene-bearing trachyte. They believe that the source area for the volcanics is a collapsed caldera centered at Guffy, Colorado.

Partially contemporaneous with and post-dating the period of intermediate-composition volcanism, another volcanic event produced what Lipman (1983) calls a transitional volcano-tectonic assemblage (transitional between subduction-related convergence and extensional rifting). Northwest-trending extensional faults were created between 30 to 20 mya and injected with small amounts of bimodal, silicic-alkalic-rhyolitic material enriched in incompatible elements. Fault development may have been influenced by a major Precambrian structural weakness similar to the Colorado mineral belt, the Jemez zone, and the Snake River Plain-Yellowstone trend. The bimodal character of the igneous rocks may be attributed to back-arc rifting caused by the slackening and sinking of the aforementioned imbricate, eastward dipping subduction zone. Lipman notes that the transitional volcano-tectonic event produced several areas of economically-significant mineralization including: Cripple Creek, Climax, Henderson, Questa, and Silverton districts.

The most recent major structural event in the southern Rocky Mountains is the development of the Rio Grande rift, accompanied by a marked change from the previous intermediate-composition volcanics to distinctly bimodal suites, including voluminous amounts of basalt (Lipman and Mehnert, 1975). The main rift system extends north-northwestward from southern New Mexico to central Colorado (Chapin, 1979) and is generally dated at 27 to 26 mya (although Tweto

(1979) contends that rift-related activity can be dated from between 40 to 7 mya). The Cripple Creek complex lies about 75 km to the east of the main rift zone. However, because it is situated between reactivated, north-northwest-trending Precambrian and/or Laramide structures (Tweto, 1979) and contains alkalic basalts, it could be associated with rifting activity. Lipman (1969) has classified rocks adjacent to the rift as alkalic basalts. Tweto (1979), however, cautions against classifying the Cripple Creek rocks without sufficient data as it is possible that they developed from contemporaneous Oligocene intermediate-composition igneous activity.

CHAPTER 3

DISTRICT GEOLOGY

Structure and Lithology

The Cripple Creek district is located within and immediately adjacent to an irregular-shaped, northwest-trending basin which developed at the intersecting contacts of the four Precambrian lithologic units described in the previous chapter. The basin, which is filled with Oligocene-age breccia, interbedded sediments, and igneous rocks, is separated into northern, southern, and eastern sub-basins by ridges of the Precambrian rock (Loughlin and Koschmann, 1935; Figs. 2 and 3). Thompson et al. (in press) have described these sub-basins as upward-flaring, individual yet coelescing breccia bodies.

The contact between the Precambrian rocks and the basin-fill (Fig. 3) generally dips 65 to 80° toward the center of the basin, but is locally either overhanging or shallow-dipping; for example, the eastern sub-basin wall dips only 23° inward (Koschmann, 1949). The walls and floor of the basin consist of a fault block mosaic. The walls are benched inward and the floor is dropped over 1 km from the present surface (Koschmann, 1949).

The dominant rock type within the basin complex is the Cripple Creek Breccia (Fig. 2). It is generally massive,

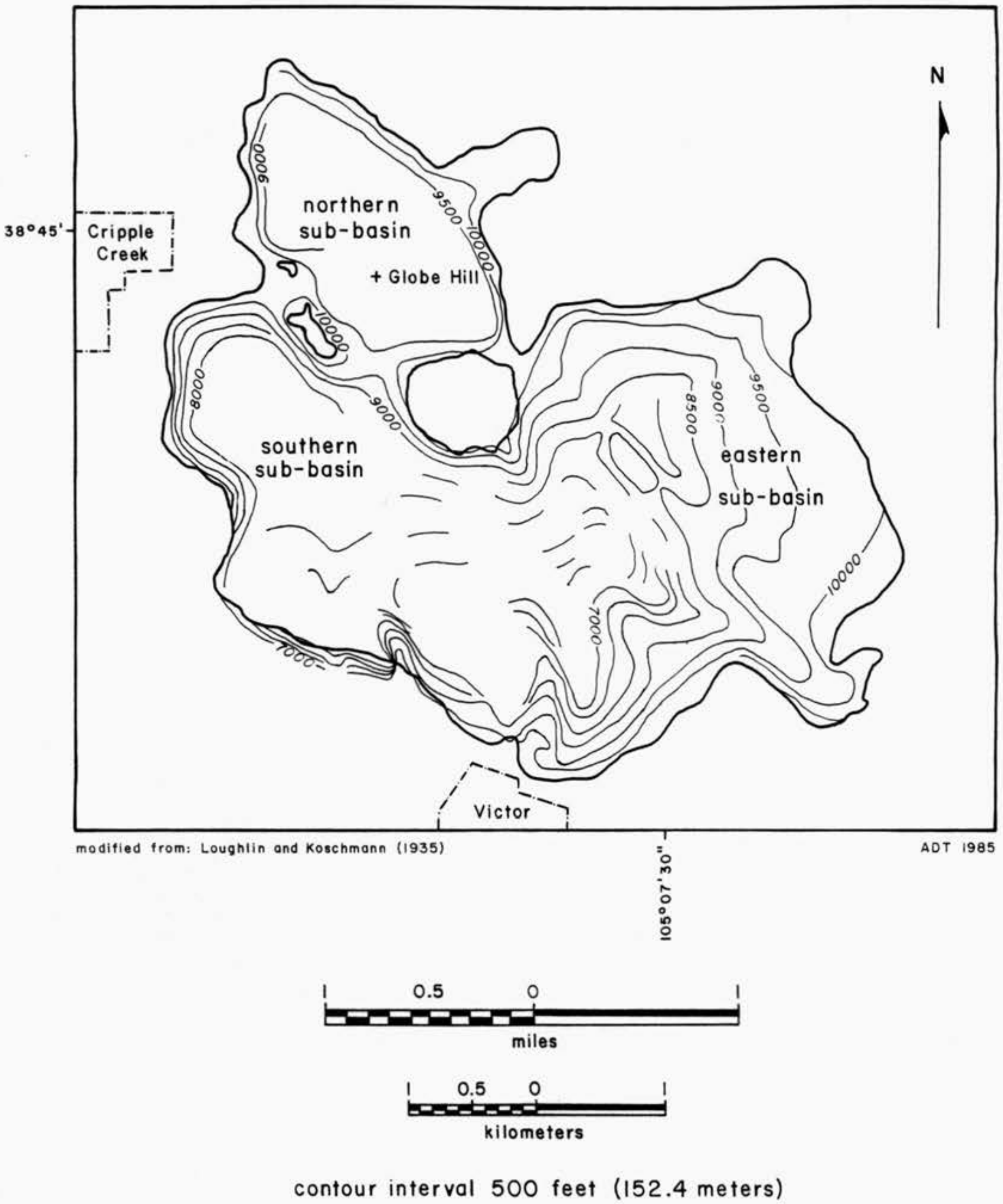

Fig. 3. Generalized elevation contours of the contact between the diatreme-intrusive complex and surrounding Precambrian rocks.

heterolithic, and has high I:F (interfragment:fragment) ratios (>1:1). The fragments are angular to subrounded, range from a few millimeters to half a meter in diameter, and are primarily composed of Oligocene igneous rocks and up to 10 percent Precambrian rocks. Near the margins of the complex, the breccia is occasionally composed entirely of Precambrian fragments (Keener, 1962). The breccia matrix consists of well-sorted quartz, microcline, and rock fragments 0.5 to 2.0 mm in diameter and lacks fine silt- or clay-size particles (Thompson et al., in press). Much of the matrix is indurated with fine-grained dolomite and pyrite (Lindgren and Ransome, 1906) and is moderately solidified into a competent unit. Accretionary lapilli and carbonized and silicified wood fragments are found within the breccia as deep as 244 m (Lindgren and Ransome, 1906).

Fluvial and shallow lucustrine sediments interbed and cap the Cripple Creek Breccia in the eastern sub-basin (Thompson et al., in press; Fig 2). The sediment section is at least 120 m thick and is comprised of conglomerate grading into a 61 m thick section of arkosic sandstone containing minor amounts of shale, clay, and limestone. These clastic sediments are almost entirely derived from the Precambrian rocks, but up to 20 percent of the fragments within the upper-most portion of arkose are composed of the Oligocene igneous rocks (Koschmann, 1941). Phonolite and latite-phonolite flows cap the arkose. This entire package is interbedded with, and buried by, the Cripple Creek Breccia.

Small blocks of similar sediments are reported in all three sub-basins, some at a depth of over 1 km (Loughlin and Koschmann, 1935). Fossil bird tracks, raindrop impressions, dessication fractures (Koschmann, 1941), leaf prints, and ripple laminations (Thompson et al., in press) suggest a subaerial to shallow lacustrine depositional environment.

The igneous rocks cutting the breccia complex occur as flow domes, dikes, irregular masses, and flat-dipping tabular bodies. Koschmann (1941) suggests that the latter may represent portions of large surface flows which are now interbedded with the breccia. The order of emplacement (earliest to youngest) of the four igneous rock types is not fully understood, but cross-cutting relationships indicate the following: latite-phonolite, syenite, phonolite, and alkali basalt (Koschmann, 1949). Lindgren and Ransome (1906) note that the phonolite and latite-phonolite were emplaced during at least two episodes as most of the breccia fragments are composed of the two rock types.

The term "latite-phonolite", introduced by Lindgren and Ransome (1906), refers to a group of alkaline igneous rocks compositionally intermediate to latite and phonolite. They are porphyritic in texture and contain phenocrysts of orthoclase, oligoclase, and sodic pyroxene in a dense phonolitic matrix. They occur as dikes, irregular masses, and flat-dipping tabular bodies within the complex (Fig. 2.).

Syenite occurs as dikes and plugs (Fig. 2). It is granular and contains the same mineral constituents as latite-phonolite with a higher mafic content (Lindgren and Ransome, 1906). Impure aegerine-augites from syenite collected on the Vindicator mine dump have been K/Ar age-dated at 33.4 ± 1 and 33.8 ± 1.3 mya (McDowell, 1971).

Phonolite, the most widespread of the four igneous rock types, occurs in a northeast-trending zone (16 km by 24 km) centered on the Cripple Creek breccia complex (Wobus et al., 1976). Within the breccia, the phonolite formed as dikes, flat-dipping tabular bodies, and plugs with minor flows (Lindgren and Ransome, 1906; Fig. 2). It is dense, gray- to light brown-colored, aphanitic, and has a trachytic texture. Its modal constituents are sodic sanidine, nepheline, analcite, aegirine-augite, and sodalite (Lindgren and Ransome, 1906). Potassium-argon dates on sanidines from a phonolite plug 4 km west of the breccia complex are 27.9 ± 0.7 and 29.3 ± 0.7 mya (Marvin et al., 1974).

Four types of alkali basalt have been reported in the Cripple Creek complex (Lindgren and Ransome, 1906). They have been termed trachydolerite, vogesite, monchiquite, and melilite basalt. All are aphanitic to strongly porphyritic and some varieties are clearly amygdaloidal (Thompson et al., in press). The alkali basalts occur as dikes which cut all other rock types in the complex. Some of these dikes formed contemporaneously with at least one late-stage breccia column exposed at the Cresson mine (Loughlin and Koschmann, 1935; Fig. 2). The breccia diatreme (Thompson et al., in press) contains cross-cutting dikes, a tuffaceous matrix, and a significant amount of breccia fragments, all composed of alkali basalt.

Ore Deposits

Ore deposits in the Cripple Creek district occur primarily as veins and mineralized breccias. Although the less abundant breccia-hosted deposits are the only economically-feasible producers today, vein deposits have historically yielded nearly all of the gold produced in the district.

Most of the vein deposits are situated near the margin of the Cripple Creek complex. The veins occur both perpendicular and concentric to the contact between the breccia and the country rocks, commonly developing at abrupt bends in this contact (Koschmann, 1949). They commonly form a step-like configuration which mimics the benched or fault-blocked walls of the complex (Loughlin and Koschmann, 1935) and occur as sheeted zones, up to 3 m across, which emmanate from major structures below 600 m (Koschmann, 1949). They are best-developed in the Cripple Creek Breccia.

Although Loughlin and Koschmann (1935) could find no evidence of mineralogical zonation in individual veins, three stages of vein mineralization were recognized district-wide. They include: stage 1) quartz-adualaria-fluorite-pyrite, stage 2) quartz-fluorite-pyrite-dolomite-celestite± base metal sulfides±calaverite, and stage 3) quartz-chalcedony-pyrite-calcite±cinnabar±fluorite±marcasite.

The El Paso vein system has been studied by Lane (1976). The veins trend parallel to dikes and small plugs of phonolite which were emplaced within a major shear zone at the contact between two Precambrian units (Fig. 2). This system has produced over 635,000 troy ounces of gold. The vein assemblages are: quartz-adularia-barite-fluorite with small amounts of pyrite, sphalerite, galena, chalcopyrite, bournonite, tetrahedrite, tennantite, calaverite, sylvanite, and molybdenite. Adularia, barite, and fluorite precipitated first, followed by quartz, and finally tellurides. Fluid inclusion homogenization temperatures for barite range from 248°C to 260°C, and for fluorite from 178°C to 190°C. Some inclusions in barite contain daughter products identified as halite crystals. The fluids which precipitated the tellurides were presumably less saline and cooler.

The vein deposits of the Ajax mine (Fig. 2) have been studied by Dwelley (1984). They occur in the Precambrian granodiorite in narrow, well-defined, sheeted zones and in the Cripple Creek Breccia in one wide zone of anastomosing, irregular veinlets. These veins have produced more than 700,000 troy ounces of gold with average grades ranging from 0.60 to 1.04 oz/t and gold:silver ratios between 23:1 and 0.2:1. Neither the gold:silver ratios nor the mineralogy are zoned, even over 1 km of vertical distance. Dwelley (1984) recognized five stages of vein mineralization. They are: stage 1) quartz-fluorite-adularia-pyrite-dolomite-marcasite; stage 2) base metal sulfides-quartz-pyrite; stage 3) quartz-fluorite-pyrite-hematite-rutile; stage 4) quartz-pyrite-rutile-calaverite-acanthite; and stage 5) quartz-fluorite-dolomite.

Fluid inclusion data have been documented by Dwelley (1984) on the first four mineralization stages in the Ajax veins. Stage 1 fluid inclusions homogenize between 206° and 510°C, are saline (33 to >40% eNaCl), contain CO_2, and indicate boiling. Stages 2 and 3 fluid inclusions homogenize at progressively lower temperatures, are less saline (0 to 8.3% eNaCl), and also indicate boiling, while stage 4 fluid inclusions homogenize below 159°C, are dilute (1.4 to 3.5% eNaCl), and indicate only intermittent boiling.

Mineralized tectonic and hydrothermal breccias, developed in the alkaline intrusions cutting the Cripple Creek Breccia, constitute the second major type of deposit in the district. These breccias host large-tonnage, low-grade (0.0X oz/t) gold mineralization, occurring as matrix-flooding and disseminations through the fragments, of which the Globe Hill deposit is an example.

Origin

Wobus et al. (1976) first suggested a diatreme origin for the Cripple Creek Breccia. Sillitoe and Bonham (1984) use the term "maar-type diatreme", but Thompson et al. (in press) describe it as a nested diatreme-intrusive complex. The authors cite as evidence of diatreme processes the overall geometry of the complex, textures of the breccia, subsidence of intact surficial organics and sediments, and the occurrence of accretionary lapilli. Experimental studies by Woolsey et al. (1975) show that fluidization resulting in a diatreme structure can generate all of these features.

Kleinkopf et al. (1970) have inferred from magnetic and gravity lows centered on the Cripple Creek complex that the alkaline igneous rocks within it originated from a large igneous mass at depth. Thompson et al. (in press) plotted the chemical composition of each igneous rock type and found three clustered groups: 1) phonolite, 2) latite-phonolite and syenite, and 3) alkali basalt. The second group may have formed by the mixing of a phonolite with an alkali basalt melt. The age and bimodal character of all three rock groups indicate that the intrusive complex may be related to extensional tectonics associated with the Rio Grande rift.

Lane (1976) and Dwelley (1984) have shown through separate fluid inclusion studies that simple cooling provided the major control on mineral deposition in the vein-type ore deposits of the district.

CHAPTER 4

HOST LITHOLOGY OF THE GLOBE HILL DEPOSIT

The geology of the Globe Hill area is shown in Plate 1. The contact between the diatreme-intrusive complex and the surrounding country rock lies one kilometer northwest of Globe Hill. Two isolated exposures, or "islands", of muscovite schist occur within the Cripple Creek Breccia to the west and southwest. The muscovite schist is classified as a member of the widespread Precambrian biotite gneiss unit discussed earlier. Underground exposures indicate that these islands are part of a large ridge which probably extends northwest from the Precambrian granodiorite island southeast of Globe Hill to the main Precambrian contact (Koschmann, 1941). This ridge separates the northern and southern sub-basins of the district (Fig. 3).

The Globe Hill deposit is hosted by a subvolcanic, pyroxene-bearing alkali trachyte porphyry (referred to district-wide as latite-phonolite) emplaced within the Cripple Creek Breccia (Fig. 4). While its geometry and extent are unknown, similar intrusive rock has been found throughout the northern sub-basin. The alkali trachyte porphyry averages less than 15 modal percent potash feldspar phenocrysts, which are composed of sanidine, high sanidine, and small amounts of orthoclase. The phenocrysts are euhedral to

Fig. 4. Pyroxene-bearing alkali trachyte porphyry from the Globe Hill deposit.

subhedral in form, equant to prismatic in cross-section, usually less than 2 mm in diameter, and are randomly oriented. Most exhibit Carlsbad twinning, and occasionally crude polysynthetic and tartan twinning.

The aphanitic groundmass consists of subhedral, prismatic feldspars less than 0.5 mm in diameter. They are generally untwinned, although some display Carlsbad twinning. X-ray diffraction studies identify the feldspars as sanidine, high sanidine, orthoclase, and small amounts of albite, all of which exhibit flow textures around some of the randomly oriented phenocrysts.

Pyroxene is a common accessory mineral occurring in trace amounts as euhedral phenocrysts less than 2 mm in diameter; smaller, euhedral grains enclosed in feldspar phenocrysts; and subhedral grains less than 0.10 mm in diameter within the groundmass.

While both the igneous texture and the mafic content vary slightly throughout the alkali trachyte porphyry, they are nowhere suggestive of separate intrusive bodies. Samples of the intrusive in diamond-drill core (DDH-500SE) immediately north of the open pit (Plate 2) show textural gradations at depth to granular alkali syenite. This may indicate the central area of the intrusive body. The seriate-textured alkali syenite contains minor accessory pyroxene, sphene, and topaz. The latter two minerals are often enclosed within the anhedral feldspar grains.

Locally, the subvolcanic mass at Globe Hill contains abundant small fragments of texturally-different alkali trachyte. Some exhibit trachytic flow alignment and others are aphanitic. A few fragments are compositionally different as well. They include mafic-rich alkali trachyte, alkali syenite, mafic-rich alkali syenite, Precambrian granodiorite, and possibly basalt.

One small alkali trachyte porphyry dike, 2 m wide, is found in the larger subvolcanic mass. It is exposed in the western portion of the open pit (Plate 2) and is apparently cut off by a major shear zone. The dike contains accessory sphene and abundant (40%) alkali trachyte porphyry fragments.

Over 150 slabbed samples representing lithologies present were stained to test for the presence of feldspathoids using a method reported by Hutchinson (1974, p. 24). The results indicate that feldspathoids are absent in the rocks examined.

CHAPTER 5

STRUCTURE AT THE GLOBE HILL DEPOSIT

Four separate structural events occurred at Globe Hill (Fig. 5). The earliest event (stage I) created a zone of hydrothermal breccia bodies which were later cut by a series of tectonic structures (stage II). Intrusive breccia (stage III), probably dike- or column-like in form, subsequently invaded a major stage II shear zone, and a separate hydrothermal breccia body (stage IV) then formed within the stage I zone. Minor readjustment occurred along the stage II faults following the four major structural events.

Stage I - Hydrothermal Breccias

The earliest hydrothermal breccias in the area occur as isolated or coelescing irregular bodies commonly found within a northwest-trending zone measuring roughly 1800 m by 700 m (Plate 1). Two large clusters of hydrothermal breccia bodies exist; one at the Globe Hill pit and another at Silver State's pit to the southeast. The breccia bodies in the Globe Hill cluster formed along pre-existing faults, at fault intersections, and at joint intersections. Each body approximates an upward-flaring column, roughly equidimensional in plan-view, but with numerous extensions outward along planar structures (Plate 2; Figs. 5, 7, and 8). The

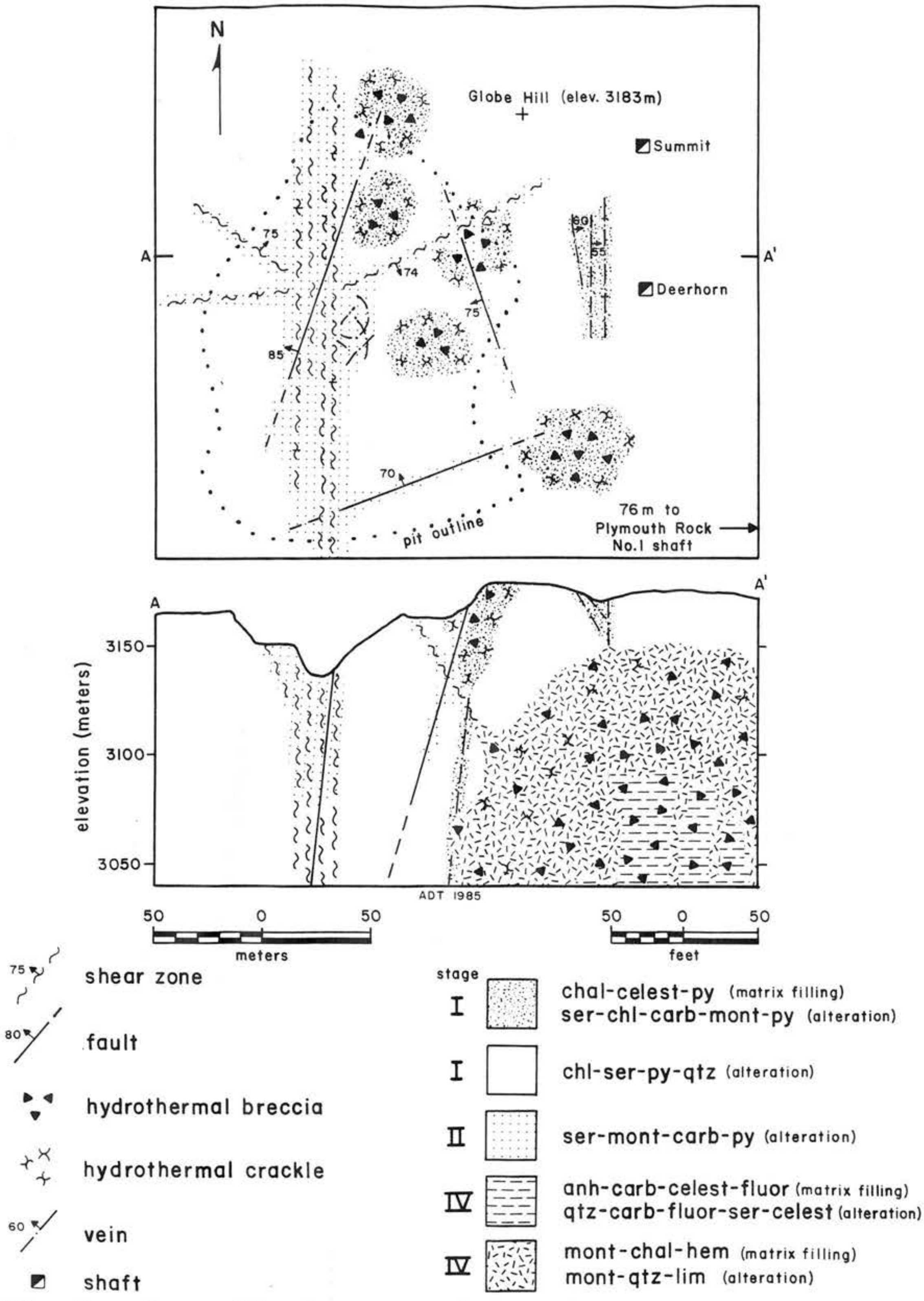

Fig. 5. Generalized map and section showing structure, mineralization, and alteration at the Globe Hill deposit.

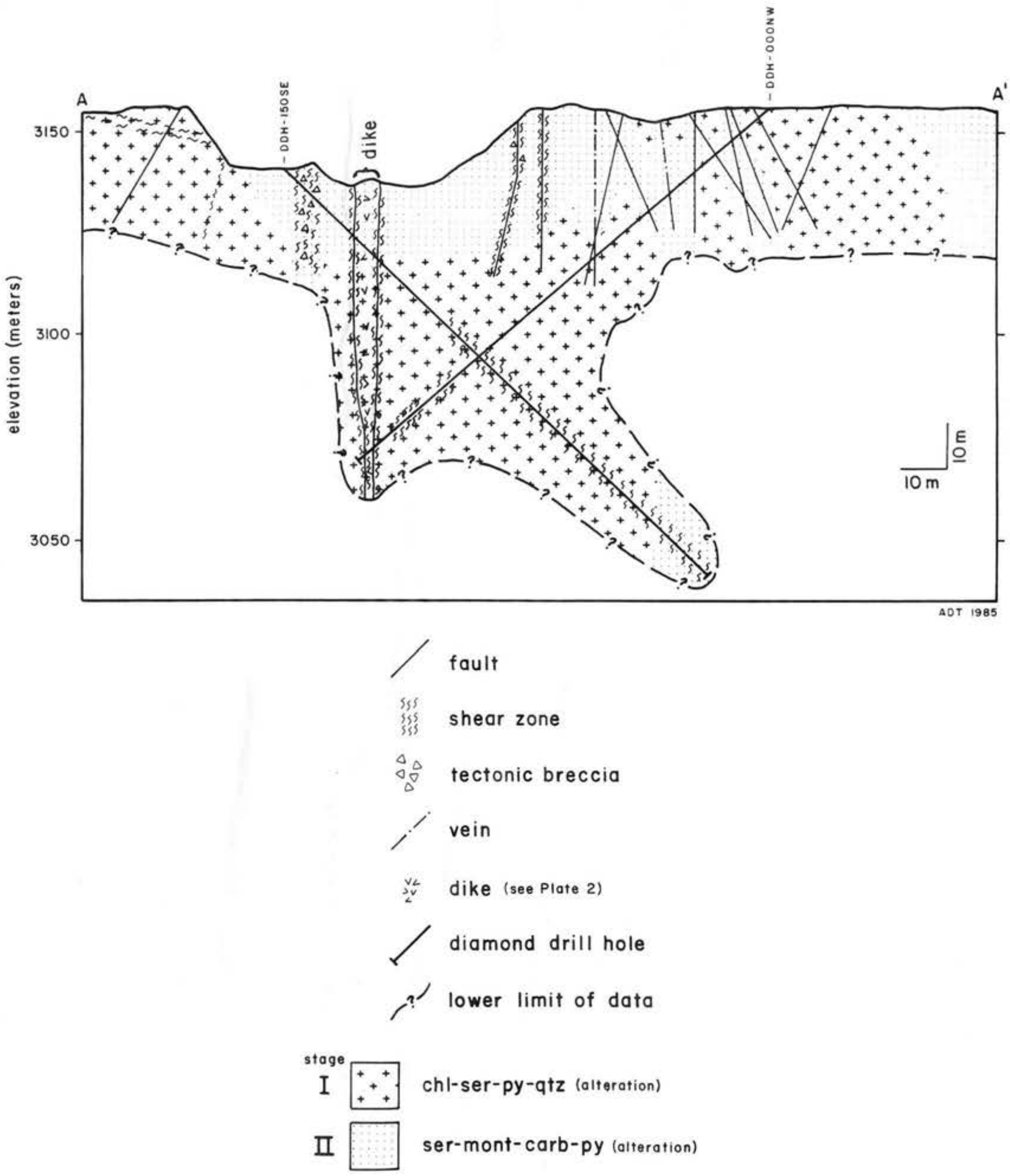

Fig. 6. Vertical cross-section A-A' (see Plate 2 for section location) showing structure, mineralization, and alteration at the Globe Hill deposit.

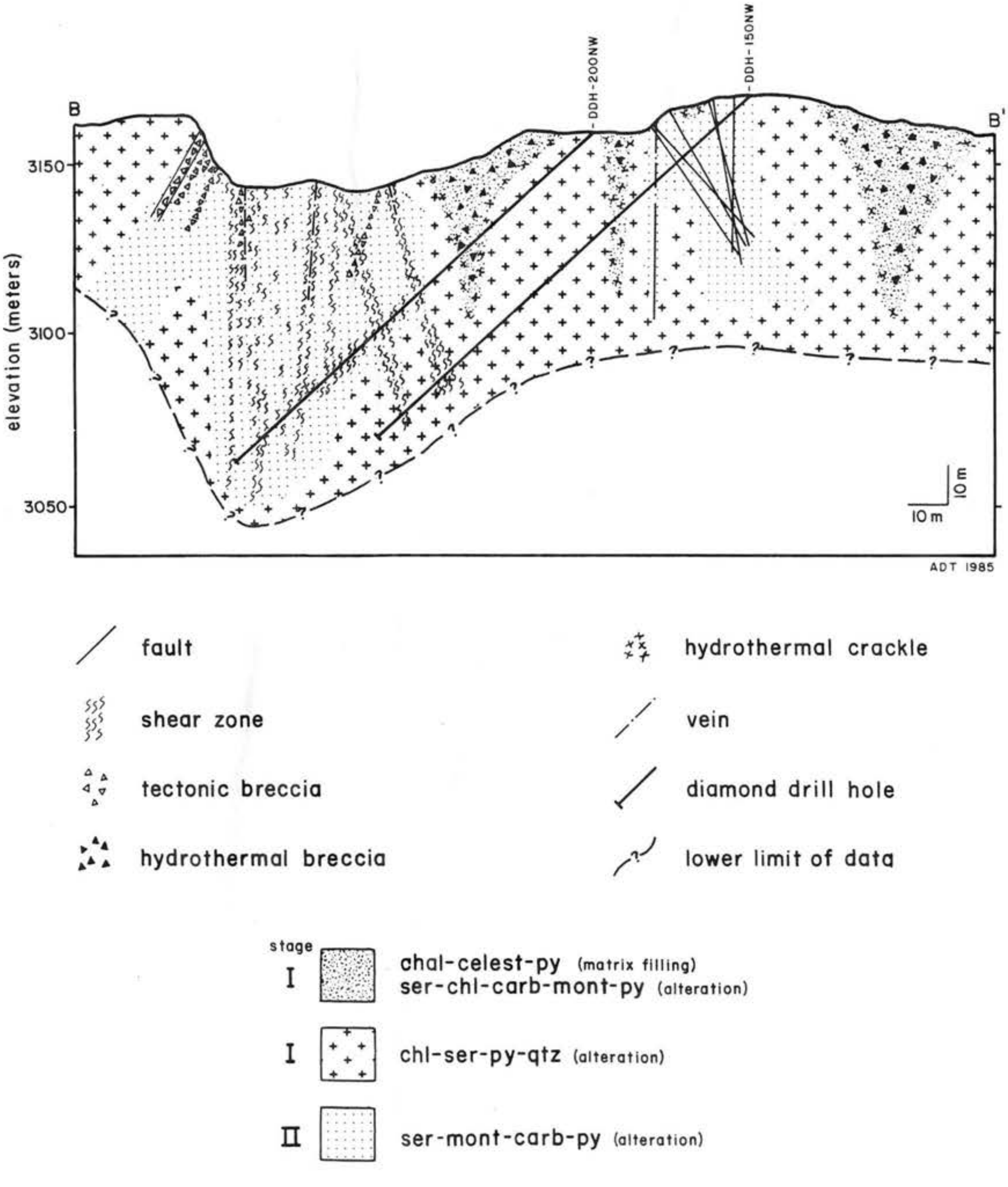

Fig. 7. Vertical cross-section B-B' (see Plate 2 for section location) showing structure, mineralization, and alteration at the Globe Hill deposit.

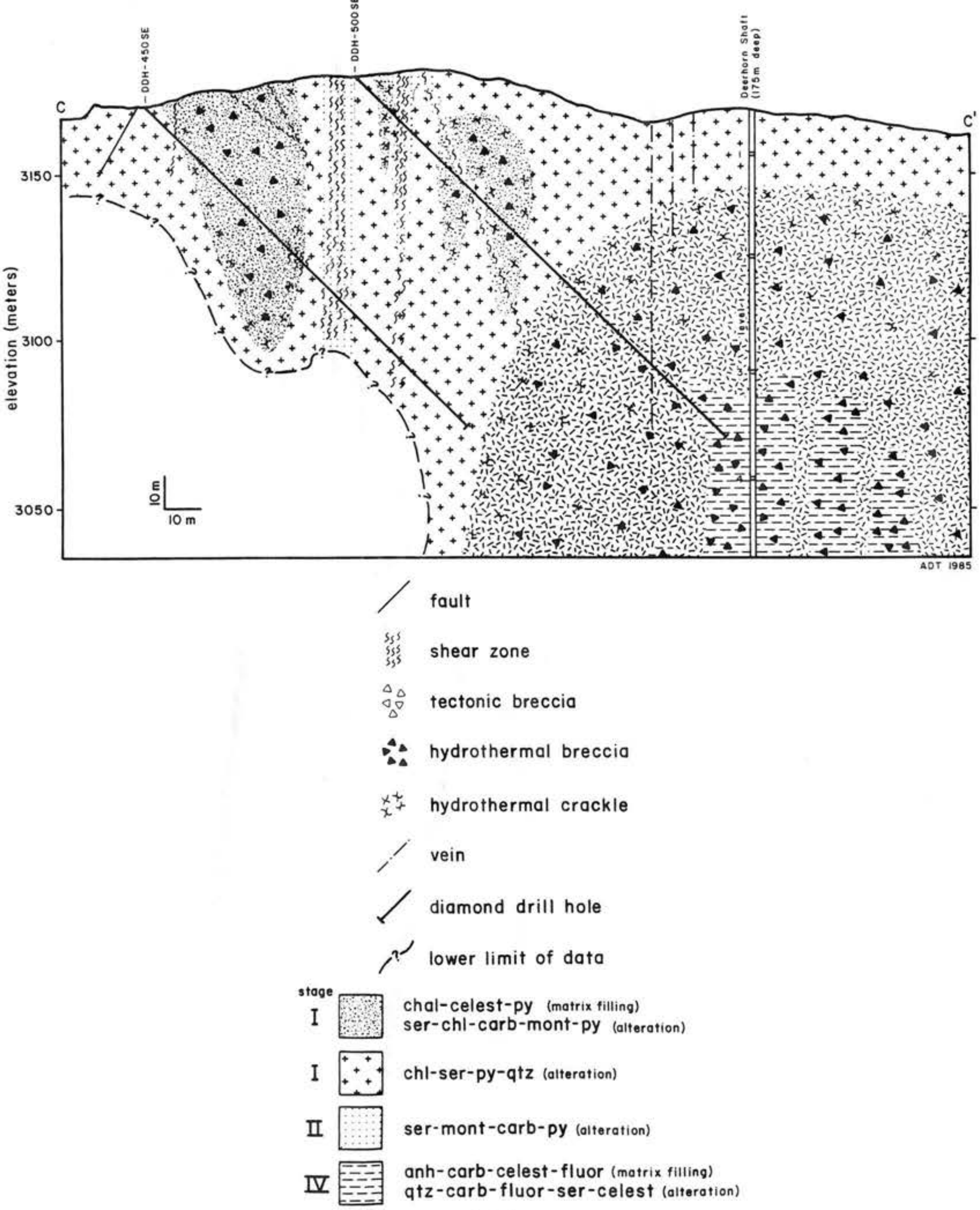

Fig. 8. Vertical cross-section C-C' (see Plate 2 for section location) showing structure, mineralization, and alteration at the Globe Hill deposit.

largest breccia body is 50 m in diameter at the surface and extends 75 m downward. The smallest breccia bodies are less than 10 cm in diameter and occur along joint intersections.

Most breccia bodies exhibit crude lateral and vertical textural zonation. They grade laterally from a breccia-dominated core, through a crackle-dominated margin, and into highly-jointed wallrock. The frequency of the joints and fractures in the wallrocks decreases outward from the breccia bodies. In vertical section, the breccia bodies appear to grade upward from a vein, to crackled and brecciated wall-rock.

Most breccia fragments range in diameter from 1 mm to 3 cm. They are generally monolithic, subangular to subrounded, poorly sorted, and grade from being fragment to matrix supported, with low (<1:3) to high (>1:1) I:F ratios. A majority of fragment compositions are identical to the immediate wallrock. They originated either as planar fragments which detached along sheeted structures, or as angular blocks derived from the crackled areas (Fig. 9). A few of the matrix-supported breccias contain fragments which have clearly been transported over a considerable vertical distance. These fragments are heterolithic, well rounded, poorly sorted, and are less than 5 cm in diameter. They are frequently composed of pyroxene-rich (up to 20%) alkali syenite, but other compositions include: biotite-rich alkali syenite, porphyritic and aphanitic varieties of mafic-rich alkali trachyte (some of which display well-developed flow

Fig. 9. Stage I hydrothermal breccia in well-jointed wallrock. Sample grades from jointed wallrock (left), to matrix-supported breccia (center), to rebrecciated fragment-supported breccia (right). Matrix is dominantly chalcedony. Note rebrecciated fragments at arrows.

textures), and quartz-fluorite vein material (Fig. 10). Accessory sphene and topaz are common in the syenitic fragments.

The breccia matrix is cemented by chalcedony and other hydrothermal minerals (discussed in chapter 6) which display open-spaced growth textures. Some of the matrix-supported breccias exhibit rebrecciation and healing textures indicative of a second episode of hydrothermal brecciation and matrix filling (Fig. 9).

Stage II - Tectonic Structures

The second structural stage is characterized by the development of steep faults and shear zones concentrated along the western edge of the stage I hydrothermal breccia zone. The most recent ore production at Globe Hill has been from this area. There are four crosscutting sub-stages of fault development. The earliest sub-stage consists of curviplanar faults concentrated near the center of the pit. These are cut by numerous steep faults and shear zones which are in turn cut by a major north-south (N-S) shear zone. The last sub-stage is represented by faults that cut all earlier tectonic structures (Fig. 5; Plate 2).

Relative displacement along the stage II tectonic structures is unclear. Marker structures, veins, and dikes cut by the N-S shear zone are not found on the opposite side, either at the surface or in core. Most of the faults, though roughly planar, are difficult to trace owing to their

Fig. 10. Stage I well-rounded, heterolithic, matrix-supported hydrothermal breccia. Sample contains fragments of mafic-rich alkali trachyte and alkali syenite, and quartz-fluorite vein material (purple). Some fragments contain fracture-controlled secondary potash-feldspar. Matrix is dominantly chalcedony.

discontinuous nature. Several faults splay along strike and dip, including the N-S shear zone, which also splays upward. Most structures have near-vertical slickensides indicating dip-slip movement. Additionally, the N-S shear zone contains horizontal slickensides suggesting lateral displacement and fault reactivation through time.

Stage II tectonic structures are usually gouge-filled, with shear and extensional joints developed in the walls. Fault breccia is locally developed along some fault surfaces and at fault intersections. Fault-induced breccia bodies are small, discontinuous, and variable in form. They are tabular- to lense-shaped along shear surfaces, and column-shaped at fault intersections. The former are most common, $\leq$0.5 m wide, and traceable up to 10 m along strike or dip.

The breccia fragments are unsorted, angular to subrounded, less than 2 cm in diameter, and supported by a gouge-filled matrix. They may be tabular- to irregular-shaped depending on the fracture pattern of the wallrock. The matrix gouge is a mixture of unsorted, very small wallrock fragments and rock flour. These fault-induced breccias have low to intermediate I:F ratios (2-3:3).

Stage III - Intrusive Breccia

The third structural event initiated emplacement of intrusive breccia. Core data from an angle hole document its presence 90 m beneath the center of the pit; it is also found as float fragments on the pit floor. The breccia occurs within the stage II N-S shear zone at the intersection of several tectonic structures. It is dike- or column-like in form and is termed "intrusive breccia."

The intrusive breccia contains unsorted, subangular to well-rounded, heterolithic fragments less than 8 cm in diameter. These fragments are matrix supported, contain I:F ratios that are intermediate to high, and are composed of aphanitic and porphyritic alkali trachyte (some of which exhibit flow texture), alkali syenite, and possibly gabbro, as well as mafic-rich varieties of each. Some fragments show evidence of having been altered prior to brecciation.

The matrix of the intrusive breccia consists of rock flour and very fine fragments, most of which are less than 1 mm in diameter (Fig. 11). Locally, the matrix is banded into alternating fragment-rich and fragment-poor zones.

Stage IV - Hydrothermal Breccia

The final structural stage at Globe Hill was one of intense hydrothermal brecciation centered near the Deerhorn shaft. The breccia body forms a vertical, round-topped, column-like mass about 220 m wide and at least 180 m deep (Argall, 1908). It has small dike- and column-like apophyses which extend outward and upward along the stage II tectonic structures (Figs. 5 and 8). Small, isolated bodies positioned above the main mass are exposed at the surface.

Texturally and compositionally, the main breccia body can be divided into two zones: a central core and a peripheral

Fig. 11. Stage III intrusive breccia with rounded, heterolithic fragments in an intensely chloritized, granular to rock flour matrix (dark green).

halo. The central core has an apex 76 m below the surface that extends at least 100 m downward and is 100 m in diameter (Argall, 1905; 1908). It contains heterolithic, subangular to subrounded, matrix-supported and often rebroken fragments (Fig. 12) up to 10 cm in size. Fragments increase in abundance from the center to the margin of the core, with corresponding I:F ratios ranging from high to intermediate. They are composed of several textural varieties of alkali trachyte porphyry (with variable degrees of pre-brecciation alteration) and broken aggregates of celesite. The matrix is entirely cemented by anhydrite and other hydrothermal minerals (discussed in chapter 6) which display open-space growth textures.

The peripheral breccia halo, about 60 m wide, consists of fragment-supported, angular to subangular wallrock fragments generally less than 2 cm in diameter and with intermediate to low I:F ratios. The breccia grades from the outer margin of this zone into crackle-dominated wallrock. It has an open matrix partially cemented by montmorillonite and other hydrothermal minerals.

Small isolated hydrothermal breccia bodies are characterized by angular to subangular wallrock fragments, usually less than 3 cm in diameter. The fragments are suspended in a matrix containing the same mineral assemblages found in the peripheral halo zone.

Breccia similar to that of the peripheral zone is also found along the last 100 m of the Chicago and Cripple Creek Tunnel (Argall, 1905; Lindgren and Ransome, 1906). This

Fig. 12. Stage IV hydrothermal breccia of the central core zone, with anhydrite matrix-filling (gray) partially weathered to gypsum (white). Note dark-colored silicified fragment (arrow).

suggests either an extension of the main stage IV breccia body southeastward to the Plymouth Rock No. 1 mine (Plate 1), or a separate body of late-stage brecciation centered nearby.

CHAPTER 6

MINERALIZATION AT THE GLOBE HILL DEPOSIT

Precious metal mineralization at the Globe Hill deposit is epithermal (as defined by Buchanan, 1981; Berger and Eimon, 1982), polymetallic, and occurs as veins, breccia-matrix fillings, and wallrock replacement bodies. It resulted from three separate hydrothermal events which coincide with three of the four structural events discussed in the previous chapter (Table 1); stage III structures are unmineralized.

Mineralization Associated with Stage I Structures

The gangue and pyrite mineralization (Table 1) of the stage I hydrothermal breccias occurs as veins, breccia-matrix fillings, and disseminations through breccia fragments and wallrock. Primary accessory oxides, tellurides, phosphates, and sulfides other than pyrite occur in trace amounts. The total sulfide content rarely exceeds a few percent.

The veins associated with stage I structures are found either as feeder conduits to, or cross-cutting the breccia bodies. They are less than 20 cm wide, continuous along strike and dip for tens of meters, and are composed of either

Table 1. Hydrothermal mineralization and alteration associated with each structural stage at the Globe Hill deposit. Minerals are listed in decreasing order of abundance for each assemblage.

	STAGE I	STAGE II	STAGE III	STAGE IV
STRUCTURES	hydrothermal breccias along early tectonic structures	tectonic faults shear zones, etc.	intrusive breccia	hydrothermal breccias
MINERALOGY	breccia matrix & veins: chalcedony quartz celestite fluorite carbonate pyrite anatase monazite sphalerite galena chalcopyrite pyrrhotite specularite rutile calaverite sericite montmorillonite	veins: quartz celestite fluorite pyrite anatase carbonate adularia galena sphalerite calaverite chalcopyrite sericite dissem. outward from gangue-free structures: pyrite anatase sphalerite galena chalcopyrite pyrrhotite specularite calaverite	granular to rock flour matrix; no mineralization	central core breccia matrix: anhydrite carbonate celestite fluorite pyrite anatase galena sphalerite chalcopyrite specularite pyrrhotite peripheral breccia matrix and veins: montmorillonite fluorite opal chalcedony hematite (spherules)
ALTERATION	breccia fragments and adjacent wallrock: sericite chlorite carbonate montmorillonite pyrite quartz apatite surrounding wallrock: chlorite sericite pyrite anatase quartz montmorillonite carbonate apatite	wallrock adjacent to veins: quartz sericite pyrite carbonate wallrock adjacent to gangue-free structures: sericite montmorillonite carbonate pyrite quartz apatite	matrix and fragments: chlorite sericite specularite hematite (spherules) quartz carbonate	fragments of central core breccia: quartz carbonate fluorite sericite celestite pyrite montmorillonite fragments of peripheral breccia and wallrock adjacent to veins: montmorillonite limonite hematite quartz

chalcedony-celestite-carbonate-fluorite-pyrite or quartz-fluorite-pyrite±celestite±carbonate. All minerals exhibit open-space growth textures.

The chalcedony-type vein assemblage predominates. It contains less than 25 percent celestite, carbonate, fluorite, pyrite, and other accessories, all of which occur as irregularly-distributed aggregates of euhedral grains sometimes aligned in crude bands parallel to the vein walls. Although they occasionally constitute the entire vein, in most cases the center is occupied by nearly-pure chalcedony. Some veins containing the entire assemblage are crosscut by veins composed entirely of chalcedony.

The quartz-type vein assemblage contains large amounts of fluorite (25-50%) and pyrite (up to 5%), and trace amounts of celestite, carbonate, and other accessories. Euhedral celestite rhombs are surrounded by xenotopic (anhedral granular) and occasionally by euhedral quartz. Quartz commonly displays undulatory extinction and "explosion" textures. Explosion textures are characterized by radiating voids within a crystal, formed when vapor bubbles, which are adhered to the crystal faces, are non-explosively displaced outward as the crystal grows (Fig. 13). The phenomenon is believed to occur only during boiling of a hydrothermal fluid (Fahley, 1981). The remaining minor mineral phases precipitated primarily within the quartz outside the explosion texture zone and occasionally interstitial to euhedral quartz crystals.

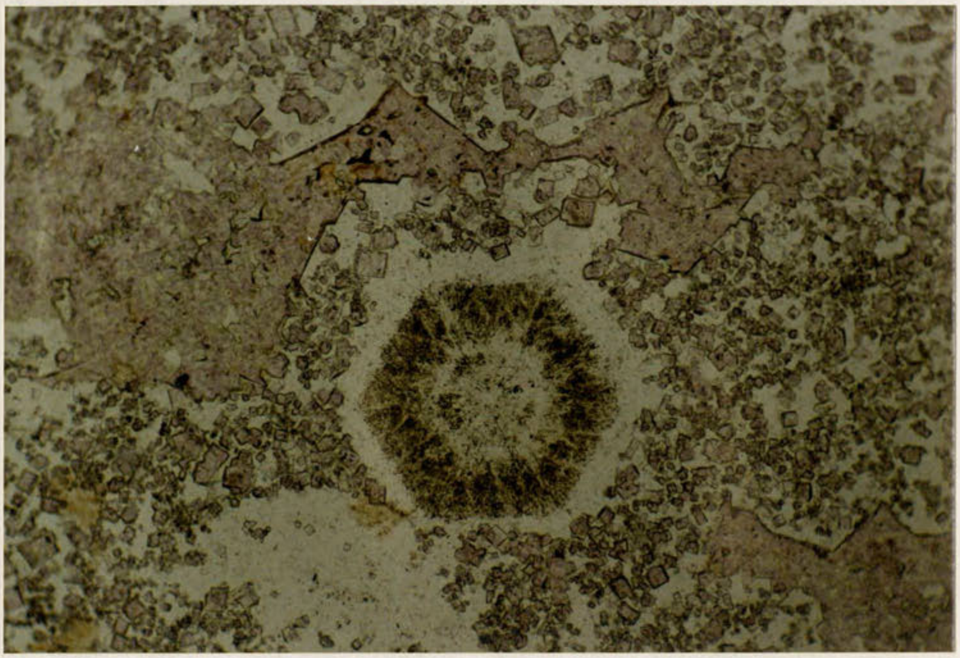

Fig. 13. Thin-section photomicrograph (plane light) of explosion texture in euhedral quartz of a stage I vein. Quartz margin intergrown with fluorite; matrix mostly fluorite. Field of view is 1.8 mm wide.

The open-space breccia-matrix filling is composed of chalcedony-celestite-pyrite$\pm$fluorite$\pm$carbonate$\pm$quartz and trace amounts of other minerals. Chalcedony constitutes over 90 percent of this assemblage. Quartz occurs in trace amounts as narrow rims surrounding fragments within the well-rounded, heterolithic variety of breccia. Trace mineral phases are randomly distributed and occur within the chalcedony in the bulk of the breccias. Vugs are lined with chalcedony in the multiple-stage breccias which also contain celestite crystals and limonite particles.

A minor amount of replacement mineralization accompanied the vein and breccia-matrix mineralization of the stage I structures. Pyrite (<5%) and other opaque accessories (trace amounts) are disseminated through the breccia fragments and within a narrow halo (<5 cm wide) in the wall-rock adjacent to the structures.

Trace amounts of anatase, monazite, sphalerite, galena, chalcopyrite, pyrrhotite, specularite, rutile, and calaverite are found within or proximal to pyrite in the mineralization related to stage I structures. Trace amounts of sericite and montmorillonite also occur in the vein and breccia-matrix assemblages.

Polished-section opaque-mineragraphy studies show that anhedral pyrrhotite, sphalerite, specularite, chalcopyrite, and calaverite, as well as euhedral specularite and rutile (all <30 μm) occur as inclusions within subhedral to euhedral pyrite crystals. Well-rounded, aggregate inclusions of chalcopyrite and pyrrhotite are also common within the pyrite.

Sphalerite, galena, and calaverite all occur as separate phases proximal to pyrite within the chalcedony or quartz gangue. Irregularly-shaped, anhedral grains and aggregates (<0.5 mm in diam) of dark-colored, high Fe sphalerite contain randomly-distributed blebs, rods, and lenses (most <5 µm in diam) of chalcopyrite. This texture is often referred to as "chalcopyrite disease". Well-rounded grains and aggregates (<3 mm in diam) of galena and subhedral to euhedral, prismatic calaverite crystals (<0.25 mm long were also identified.

Anatase, which showed strong intensity Ti peaks and possibly minor Fe peaks on a JEOL Superprobe 733 with Tracor Northern EDS, was identified in polished section. The anatase occurs as anhedral, irregular grains (<10 µm in diam) and aggregates (<0.2 mm in diam) closely associated with pyrite. Many samples exhibit partial replacement of pyrite by anatase (Fig. 14). Anatase was found in trace amounts in all three mineralization types associated with stage I structures.

A similar method was used to identify monazite. EDS analysis results show strong La, Ce, and P peaks, and thin-section study confirmed the presence of monazite. It occurs as small (<40 µm), prismatic, euhedral to subhedral, individual crystals which are often totally enclosed by anatase

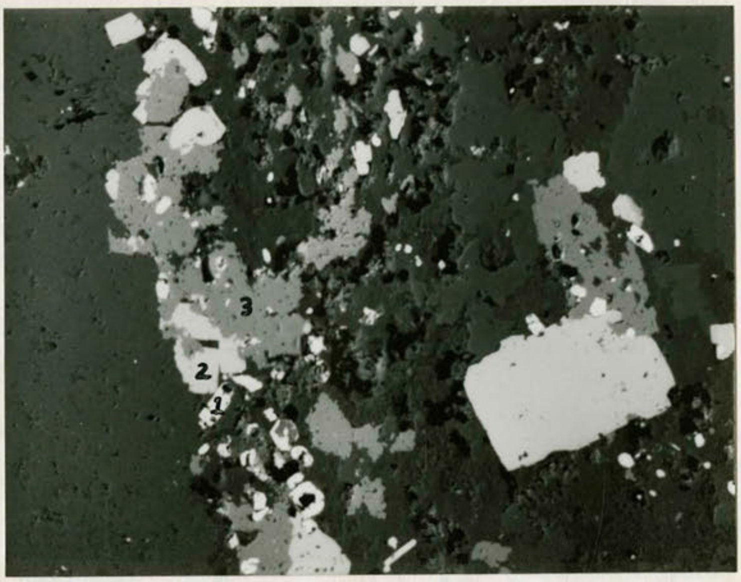

Fig. 14. Back-scattered electron image from a polished-section of stage I replacement mineralization in a breccia fragment. Sample shows monazite (1: white, subhedral, prismatic crystals), pyrite (2: gray-white, rectangular crystals), and anatase (3: gray, irregular aggregates) in altered wallrock (dark gray and black). Pyrite is partially replaced by anatase. Field of view is 0.62 mm wide.

or partially enclosed by pyrite (Fig. 14). Monazite was found disseminated through breccia fragments, and probably occurs in vein and breccia-matrix fillings of stage I structures as well.

Cross-cutting relationships, partial enclosures, rims, and partial replacements indicate that celestite precipitated first, followed by quartz$\pm$fluorite, chalcedony$\pm$ fluorite, fluorite, monazite, pyrite, galena$\pm$sphalerite, sphalerite, carbonate, chalcedony$\pm$celestite, and late celestite (Fig. 15). Calaverite appears to have precipitated after fluorite and before pyrite.

Mineralization Associated with Stage II Structures

The gangue and pyrite mineralization of the stage II tectonic structures occurs as veins and disseminations through wallrock adjacent to structures which crosscut the veins. Primary accessory oxides, tellurides, and sulfides other than pyrite (Table 1) occur in trace amounts. The total sulfide content is less than five percent. Both types of mineralization have been strongly oxidized, making paragenetic relationships difficult to ascertain (Fig. 15).

Multiple episodes of vein development are found mainly within a 15 m by 45 m area now exposed near the center of the pit (Fig. 5; Plate 2). The veins occur as discontinuous, cymoid-like lenses (<20 cm wide) of variable strike and dip. Compositions consist of quartz-celestite-fluorite-pyrite$\pm$ carbonate$\pm$adularia with trace amounts of anatase,

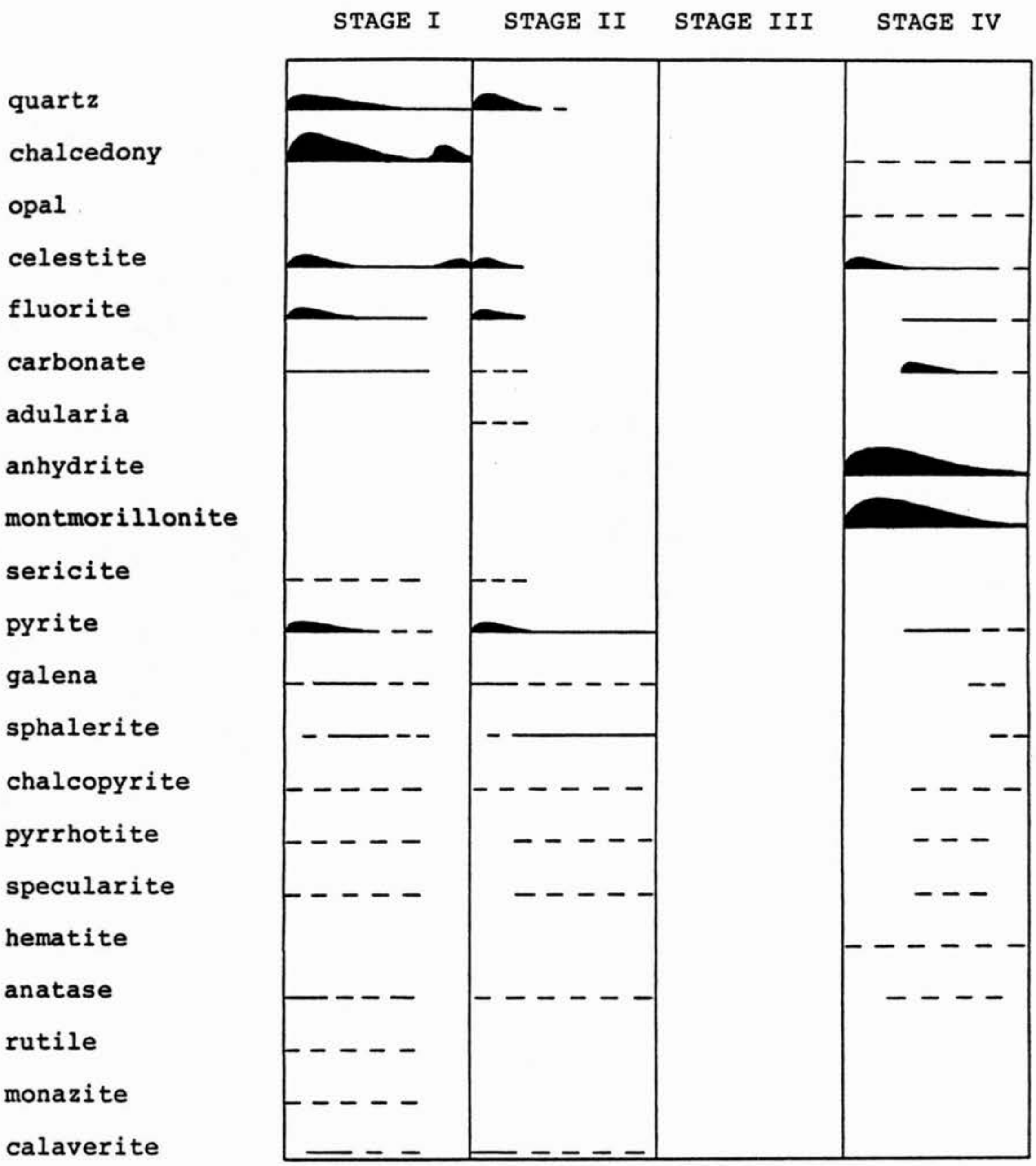

Fig. 15. Generalized paragenetic diagram of mineralization associated with each structural stage at the Globe Hill deposit. Width of lines show relative abundances; dashed line indicates sporadic deposition.

galena, sphalerite, calaverite, chalcopyrite, and sericite. All of these minerals exhibit open-space growth textures. Quartz constitutes over 95 percent of the vein material and exhibits undulatory extinction. Explosion textures are found within the quartz in a narrow zone adjacent to the vein margins (Fig. 16). All of the accessory minerals precipitated within this zone, although celestite also occurs outside the zone. Adularia rhombs are often found attached directly to the wallrock (Fig. 17).

Disseminated mineralization occurs in the wallrock adjacent to structures which crosscut the first mineralization type. Pyrite and trace amounts of anatase, sphalerite, chalcopyrite, pyrrhotite, specularite, and calaverite occur in a halo less than 3 m wide. Halos adjacent to shear zones have developed up to 10 m in width (Fig. 5; Plate 2). The structures themselves are commonly unmineralized, other than small amounts of pyrite. Polished-section mineragraphy studies show that pyrite occurs as subhedral to euhedral grains and aggregates (0.1 mm avg diam) which contain well-rounded inclusions (<20 µm in diam) of pyrrhotite and specularite. Anatase occurs as irregular, anhedral grains and aggregates (<0.1 mm in diam) which rim and partially replace pyrite. Sphalerite with chalcopyrite disease occurs as irregular, anhedral grains and aggregates (<0.1 mm in diam). Several rounded, anhedral grains of galena (<50 µm in diam) were observed in one sample, and one small (<5 µm long), subhedral, prismatic calaverite crystal was identified.

Fig. 16. Quartz vein along early-formed stage II tectonic structure. Narrow white band along vein margin is a zone of explosion texture which contains sulfides, oxides, and telluride coprecipitated with quartz. Yellow stain on wallrock due to sodium cobaltinitrite.

Fig. 17. Thin-section photomicrograph (X-nicols) of a quartz vein along an early-formed stage II tectonic structure. Fracture in wallrock (dark aggregate) is rimmed by adularia (dark gray rhombs), and filled with quartz (white and light gray). Field of view is 0.6 mm wide.

Mineralization Associated with Stage IV Structures

The gangue and pyrite mineralization of the stage IV hydrothermal breccia body (Figs. 5 and 8) occurs as breccia-matrix filling of the central core zone and the peripheral halo. Primary oxides and sulfides including pyrite occur in trace amounts (Table 1), and the total sulfide content is low (<1%).

The open-space breccia-matrix filling of the central core zone is composed of anhydrite-carbonate-celestite-fluorite and trace amounts of pyrite, anatase, sphalerite, galena, chalcopyrite, specularite, and pyrrhotite. Trace amounts of the oxides and sulfides are also disseminated in irregular, narrow halos (<3 mm wide) within the breccia fragments.

Anhydrite constitutes over 90 percent of the assemblage and occurs as subhedral to euhedral, fan-shaped, bladed aggregates (1 mm avg length) which commonly display curved cleavage planes and crystal faces (Fig. 18). Celestite (<5%) is found as euhedral rhombs (<0.5 mm wide) and broken xenomorphic aggregates (<10 mm in diam) within the anhydrite aggregates. Most celestites are partially replaced by anhydrite and all other minerals along grain boundaries and cleavage planes, and large crystals occasionally exhibit crudely-developed explosion texture. Spheroidal carbonate (<50 μm in diam; <5%), euhedral fluorite cubes (0.1 mm wide; <2%), and trace amounts of the opaque minerals occur together in bent, folded, or broken, sinuous aggregates

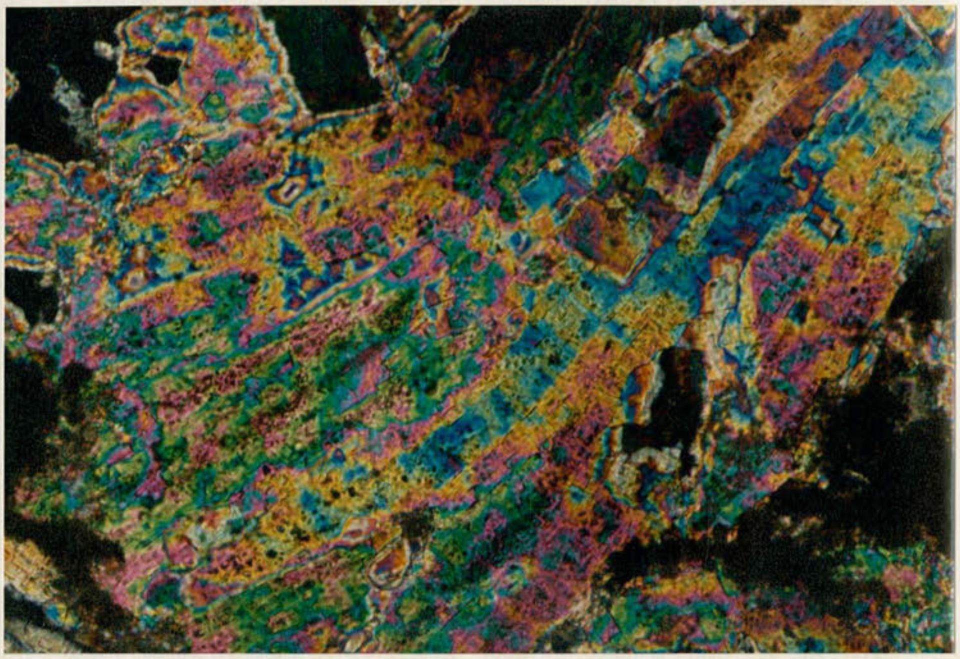

Fig. 18. Thin-section photomicrograph (X-nicols) of fan-like aggregates of bladed anhydrite in stage IV central core zone breccia matrix. Note the curved cleavage planes and crystal faces, and the planes of abundant fluid inclusions (dark specks). Field of view is 0.25 mm wide.

interstitial to and partially replacing the anhydrite aggregates. The opaques consist primarily of subhedral to euhedral pyrite grains and aggregates (<2 mm in diam) which often contain inclusions of anhedral, prismatic chalcopyrite; subhedral, lath-shaped specularite (both <30 µm long); and occasionally anhedral, rounded pyrrhotite (<10 µm in diam). Anatase occurs as irregular, anhedral grains and aggregates (<0.2 mm in diam), some of which have partially replaced pyrite. Anhedral to subhedral, rounded grains and aggregates (<0.5 mm in diam) of galena often display curved cleavage planes, and anhedral, irregularly-shaped grains and aggregates (<0.2 mm in diam) of sphalerite exhibit chalcopyrite disease. The chalcopyrite also occurs as individual, anhedral, irregularly-shaped grains and aggregates (<50 µm in diam).

Mineral textures such as rimming, partial enclosure, and partial replacement indicate that celestite precipitated first, followed by anhydrite. Paragentic relationships between carbonate, fluorite, and the opaques are unclear, but opaque mineragraphy studies indicate that pyrite$\pm$chalcopyrite$\pm$specularite$\pm$pyrrhotite precipitated prior to anatase and galena$\pm$sphalerite, followed by sphalerite$\pm$galena, and finally chalcopyrite (Fig. 15).

The stage IV peripheral halo is composed of fragment-supported hydrothermal breccia partially cemented by massive montmorillonite. Montmorillonite is white, limonitic brown, or brilliant yellow-green in color. It contains minor amounts of opaline to chalcedonic quartz and hematite spherules (<1 mm in diam), and is crosscut by narrow fluorite veinlets. Although neither anhydrite nor gypsum were found in a core hole which penetrates the breccia, Cross and Penrose (1895) report occurrences of gypsum-coated seams and fragments directly above the central core zone. Montmorillonite from the peripheral breccia halo also extends outward along stage II tectonic structures.

CHAPTER 7

ALTERATION

Five separate alteration events have been recognized at the Globe Hill deposit. Each of the first four types is hypogene and related to one of the major structural stages discussed in chapter 5 (Table 1). The fifth type is related to supergene weathering. The last hypogene event and subsequent supergene weathering formed extensive, overlapping oxidation zones. The alteration of the deposit is generally moderate, and the groundmass of the alkali trachyte porphyry host rock is in each case more highly altered than the phenocrysts.

Alteration Associated with Stage I Structures

Fragment alteration within stage I hydrothermal breccia bodies is zoned. Each fragment contains weak to moderate, disseminated sericite-chlorite-carbonate-montmorillonite-pyrite±quartz±apatite alteration (Figs. 5, 7, and 8; Plate 2) surrounded by a rind (<0.5 mm wide) of intense sericite-pyrite-quartz±carbonate alteration. Some fragments exhibit an irregular silicification rind around their outer margins (<0.1 mm wide).

Wallrock alteration bordering the hydrothermal breccia bodies and feeder veins is also zoned. The breccia bodies and veins are ringed by a halo (<5 cm wide) of weak to moderate sericite-chlorite-carbonate-montmorillonite-pyrite± quartz±apatite alteration. A moderate chlorite-sericite-pyrite-anatase-quartz±montmorillonite±carbonate±apatite alteration pervades the wallrock surrounding these halos (Fig. 19), although the extent of it has not been delineated (Fig. 5; Plate 2). Chalcedony veinlets, found erratically distributed throughout the wallrock, display a narrow halo (<0.2 mm wide) of intense sericitization and an outer halo (<0.5 mm wide) of strong chloritic alteration grading outward to the pervasive assemblage.

Alteration Associated with Stage II Structures

Wallrock alteration adjacent to the stage II tectonic structures is of two types. The early, vein-filled structures are surrounded by narrow, quartz-sericite-pyrite-carbonate alteration halos (<5 cm wide) of moderate intensity. Sericite-montmorillonite-carbonate-pyrite±quartz± apatite alteration of weak to moderate intensity (Fig. 20) penetrated the wallrock surrounding the later, gangue-free, cross-cutting structures up to 10 m (Figs. 5-7; Plate 2). It extends to a depth of 100 m in the major N-S shear zone and to shallower depths in the narrower structures (Figs. 5-8). No chlorite-dominated assemblage has been recognized in either alteration type.

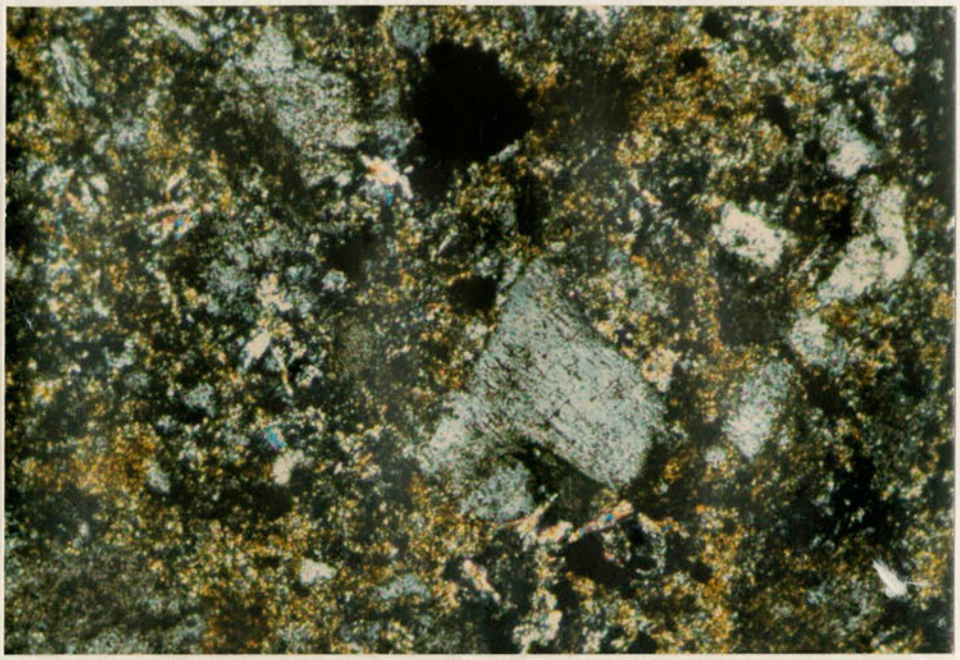

Fig. 19. Thin-section photomicrograph (X-nicols) of stage I chlorite (fine-grained green-gold)-sericite (coarser, brilliant blades)-pyrite (opaque) alteration of wallrock (gray phenocrysts and groundmass) which surrounds the hydrothermal breccia bodies. Field of view is 1.8 mm wide.

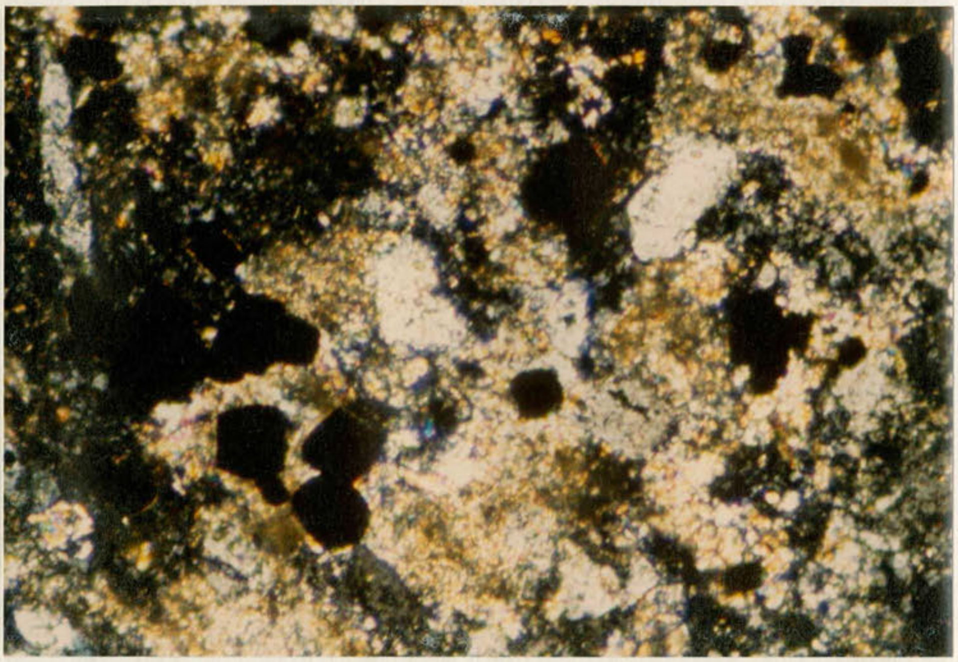

Fig. 20. Thin-section photomicrograph (X-nicols) of sericite (fine-grained, brilliant)-montmorillonite-carbonate-pyrite (opaque) alteration of wallrock (gray) adjacent to gangue-free stage II tectonic structures. Field of view is 2.0 mm wide.

Alteration Associated with Stage III Structures

Alteration of the stage III intrusive breccia body affected both fragments and matrix. Most fragments display a weakly disseminated, chloritic alteration encircled by a narrow rind (<1 mm avg width) of chlorite-sericite-hematite-quartz-carbonate alteration. The intensity of the alteration rind ranges from moderate to strong depending upon the primary fragment composition and texture. Matrix alteration is similar to that of the fragment margins although no carbonate has been identified. Hematite occurs in both cases as blades (specularite) and as spherical aggregates. A few breccia fragments contain fracture-controlled adularia and intense quartz-sericite alteration.

Alteration Associated with Stage IV Structures

The stage IV alteration types correspond to the major structural zones of the stage IV hydrothermal breccia body. The heterolithic fragments of the central zone contain quartz-carbonate-fluorite-sericite-celestite-pyrite-montmorillonite alteration (Figs. 5 and 8) of moderate intensity. Some of these fragments are narrowly rimmed (<3 mm wide) by an intense pyrite-fluorite-carbonate alteration. The wallrock fragments constituting the peripheral halo zone have been altered to an assemblage of montmorillonite-quartz-limonite (Figs. 5 and 8). Alteration intensity increases with proximity to the central core zone. The oxidation of pre-existing sulfide and telluride mineralization increases within the peripheral halo toward the completely unoxidized core zone, while the percentage of pre-breccia sulfide casts remains constant at a trace. The relationships between the montmorillonite alteration, degree of oxidation, and sulfide content of the peripheral zone were also reported in the Deerhorn workings by Argall (1905, 1908). The geometry of the oxidation and the occurrence of hematite spherules within the montmorillonitic matrix of the peripheral zone, suggest a possible hypogene origin for this unusual oxidation.

Stage IV alteration overlaps that of stage II where the peripheral halo zone extends along pre-existing gangue-free stage II tectonic structures. Fragments were cemented by montmorillonite during stage IV mineralization, and fragments and adjacent wallrock were simultaneously altered to a weak montmorillonitic assemblage.

Supergene Weathering

Supergene weathering has partially oxidized the Globe Hill deposit to a depth of at least 270 m (45 m below the Chicago and Cripple Creek Tunnel; Lindgren and Ransome, 1906). The effects of weathering are most pronounced in stage I hydrothermal breccias and stage II tectonic structures, where permeability has been sufficient to allow for downward percolation of oxidizing surface water. Little remobilization of precious metals accompanied the weathering process.

The reactions of anhydrite, pyrite, galena, chalcopyrite, and calaverite to oxygenated surface waters produced gypsum, limonite, anglesite, covellite, and native gold, respectively. Carbonate dissolution may be responsible for the formation of wad, pyrolusite, and manjiroite (hydrated sodium-potassium-manganese oxide) which occur as fracture-coatings throughout the deposit. Autunite (hydrated calcium-uranium phosphate) was identified in several weathered stage I veins. Celestite often accompanies iron/manganese oxide fracture fillings and is due to the weathering of mineralized stage I veins and breccias and stage II veins.

The composition and relative proportions of minerals produced by supergene weathering depend largely upon the original sulfide content and degree of oxidation. Weathering of stage I hydrothermal breccias produced an assemblage of limonite-goethite-manjiroite-wad$\pm$hematite$\pm$jarosite$\pm$celestite$\pm$autunite. Weathering of stage II tectonic structures produced hematite-jarosite-limonite-geothite-manganese oxides$\pm$ celestite. Weathering of the stage IV hydrothermal breccia body produced gypsum$\pm$limonite.

CHAPTER 8

GEOCHEMISTRY

Geochemical data collection at Globe Hill was accomplished by two methods. Selected rock samples were collected from mineralized and altered areas of the pit and geochemically analyzed for a suite of metallic trace elements. Fluid inclusion microthermometry and crushing studies were conducted on specific gangue minerals associated with stage I, II, and IV structures. Although both data sets are preliminary, they are qualitatively useful and will aid in the development of a genetic model for the deposit.

Trace Elements

Fifty-three rock chip and channel samples (about 1 kg each; Plate 2) were submitted to Bondar-Clegg, Inc. (Denver) for quantitative trace element analysis. After the samples were dried, the bulk of each was pulverized to -80 mesh and split four ways. Three of these splits were analyzed for various elements using an atomic absorption method and were treated in the following manner: the first split was digested in aqua regia and analyzed for Ag, Cu, Pb, Zn, Mo, Co, Cd, and Ni; the second was either digested totally in hydrofluoric acid or was fused and analyzed for Au and V; and the third was digested using an unreported, "specific" technique and analyzed for Te. The fourth split was digested in a nitric-perchloric solution and analyzed for As using a colorimetry method. A small portion of each sample was pulverized to -35+30 mesh and analyzed for Sb using X-ray fluorescence.

The results of the quantitative trace element analyses are given in Table 2. Observation of the data reveals a few of the more important trends. Stage I and II mineralized structures contain higher Au values than do those of stages III and IV. The Ag/Au ratios are, in general, greater than 2:1, but can be as low as 0.03:1 in zones of significant gold mineralization. Although silver-bearing tetrahedrite (Lindgren and Ransome, 1906) and acanthite (Dwelley, 1984) are found elsewhere in the district, no silver-bearing mineral was identified to account for the relatively high Ag values (>10 ppm) in several samples. The Pb values are generally higher than Zn, but a high galena weathering rate could account for the low ratio of galena to sphalerite observed in the samples. Roscoelite, a vandium-rich sericite, has also been reported district-wide (Lindgren and Ransome, 1906). While none was identified at Globe Hill, the abundant sericite may be the source of high V values.

Valid statistical treatment of the trace element data is not possible for several reasons. There are not enough samples (<100) to accurately calculate threshold values using the graphical method of Sinclair (1974). Also, the rock samples are not representative of the entire deposit, as

Table 2. Trace element content of selected rock samples from the Globe Hill deposit. Abbreviations are defined at end of table. Please refer to Plate 2 for sample locations, and to Chapter 8 for analytical procedures.

		(PPM)													
		Au	Ag	As	Sb	Te	Cu	Pb	Zn	Mo	Co	Cd	Ni	V	Ag/Au
83GH- 1	oxy stg II sh	1-10	1-10	26	89	7.0	51	1060	185	590	12	1.1	<2	203	6.85
- 3	part-oxy stg II vn	1-10	> 10	14	1100	22.5	31	2580	45	2500	2	<0.2	<2	298	6.23
- 4	oxy stg II fault gouge	< 1	1-10	19	< 2	0.8	52	495	94	465	2	0.2	<2	97	2.28
- 5	oxy stg II vn	< 1	< 1	7	< 2	0.4	16	139	89	46	1	0.3	<2	38	1.33
- 6	stg IV mont-filled bxa	< 1	< 1	5	< 2	<0.2	9	118	655	17	5	<0.2	4	41	7.50
- 7	oxy stg II alt	< 1	1-10	16	< 2	1.5	13	372	40	40	1	<0.2	<2	76	2.67
- 8	stg IV mont-filled bxa	1-10	1-10	180	3	2.5	27	540	276	267	1	<0.2	<2	89	0.59
- 9	oxy stg II fault bxa	1-10	1-10	12	< 2	<0.2	41	220	105	37	<1	<0.2	<2	67	1.91
-10	unoxy stg I bxa	< 1	1-10	18	< 2	2.0	52	324	35	204	5	<0.2	<2	65	4.67
-11	oxy stg II vn	< 1	1-10	22	< 2	2.5	21	1670	85	91	3	<0.2	<2	90	1.95
-12	stg IV mont-filled bxa	1-10	< 1	52	3	1.5	27	400	160	39	2	1.0	2	106	0.33
-13	oxy stg II alt	< 1	< 1	11	< 2	1.0	8	211	93	27	1	0.2	<2	79	2.67
-14	oxy stg II fault bxa	1-10	1-10	29	18	13.5	25	1780	41	156	2	<0.2	<2	49	3.59
-15	unoxy stg I alt	< 1	< 1	6	< 2	0.4	16	31	333	5	22	<0.2	1	125	1.08
-16	stg I vnlets	< 1	< 1	6	< 2	0.2	12	58	129	11	2	<0.2	<2	60	0.42
-17	oxy alk trach porph dike	< 1	< 1	19	< 2	0.6	4	119	34	27	<1	<0.2	<2	41	3.03
-18	unoxy stg I alt	< 1	< 1	4	< 2	0.2	10	24	83	4	1	<0.2	<2	91	3.33
-19	unoxy stg I vnlets	< 1	< 1	4	< 2	0.4	15	156	23	27	<1	<0.2	<2	47	12.31
-20	oxy stg II sh	< 1	1-10	26	24	3.0	26	765	81	74	2	<0.2	<2	95	4.87
-21	oxy stg II alt	< 1	1-10	27	< 2	1.0	21	56	93	92	1	<0.2	<2	73	4.86
-23	stg IV mont-filled bxa	< 1	< 1	15	< 2	1.0	14	111	35	77	2	<0.2	<2	90	0.91
-24	oxy stg II alt	< 1	< 1	7	< 2	0.4	12	32	67	27	1	<0.2	<2	107	1.67
-25	part-oxy stg I alt	< 1	< 1	7	< 2	0.4	33	48	57	17	2	<0.2	<2	100	0.78
-26	oxy stg II alt	< 1	< 1	8	< 2	0.4	17	221	35	104	1	<0.2	<2	80	0.98
-27	5' channel across oxy stg II sh	1-10	< 1	32	10	1.0	56	500	170	252	2	0.7	4	151	0.15
-30	SAA w/ abndnt stg II vein frags	1-10	1-10	27	32	5.5	35	460	115	630	<1	0.9	3	191	1.01
-32	stg II vn	> 10	1-10	5	44	15.5	8	127	19	27	1	0.2	<2	24	0.05
-33	stg III mont w/in vn	1-10	< 1	21	21	1.5	156	345	309	158	9	2.0	14	172	0.08
-34	5' channel across oxy stg II sh	> 10	1-10	18	17	33.0	13	96	23	62	1	0.4	<2	42	0.03

Table 2, Continued

	Au	Ag	As	Sb	Te	Cu	Pb	Zn	Mo	Co	Cd	Ni	V	Ag/Au
-35 oxy stg II alt	< 1	< 1	31	< 2	1.0	17	48	26	57	1	<0.2	<2	79	0.65
-36 part-oxy stg II vn	< 1	< 10	15	< 2	1.5	40	2530	136	290	22	0.4	<2	47	15.21
-37 oxy stg II fault gouge	1-10	1-10	49	< 2	2.5	13	347	44	155	4	0.2	<2	74	0.56
-38 5' channel across oxy stg II sh	1-10	< 1	37	< 2	0.8	56	670	177	104	7	2.0	<2	118	0.55
-39 SAA	> 10	1-10	98	< 2	6.5	35	950	70	400	3	0.3	2	97	0.06
-40 SAA	< 1	1-10	15	< 2	0.4	24	304	192	147	1	0.3	3	133	1.65
-41 oxy stg II sh	< 1	< 1	12	< 2	0.4	16	284	63	64	1	<0.2	<2	59	1.54
-42 oxy stg II alt	< 1	< 1	18	< 2	0.4	15	39	23	32	<1	0.3	<2	72	1.71
-43 part-oxy stg I alt	< 1	< 1	3	< 2	<0.2	19	29	171	4	5	0.4	2	109	1.43
-44 stg IV mont-filled bxa	< 1	< 1	18	< 2	<0.2	134	133	1180	28	32	2.3	15	48	2.61
-45 unoxy stg I vn	< 1	< 1	5	< 2	<0.2	7	222	39	24	<1	<0.2	<2	24	2.40
-46 supergene MnOx-FeOx	< 1	1-10	29	< 2	<0.2	35	45	1060	97	90	1.5	7	20	2.45
-47 part-oxy stg I alt	1-10	1-10	150	13	2.5	44	209	29	69	2	0.3	<2	306	0.30
-48 unoxy stg I bxa	< 1	1-10	9	< 2	0.4	102	190	122	91	6	2.2	<2	60	8.89
-49 oxy stg II sh	< 1	1-10	9	< 2	0.8	144	1070	850	350	12	5.4	10	68	4.63
-50 oxy supergene jsp flt	< 1	< 1	28	< 2	<0.2	19	141	119	20	<1	1.4	<2	63	3.40
-51 oxy stg I bxa flt	< 1	< 1	25	< 2	0.6	40	96	162	95	3	0.6	<2	80	3.08
-52 part-oxy stg I vn flt	1-10	< 1	15	< 2	0.6	12	217	223	44	<1	0.5	<2	29	0.36
-53 unox stg I crackle	< 1	1-10	29	< 2	0.4	94	46	83	27	9	13.0	3	98	2.33
-54 unox stg I bxa	1-10	1-10	31	< 2	7.5	59	233	327	93	10	12.0	3	68	0.92
-55 oxy stg I vn flt	> 10	1-10	39	50	8.5	52	162	91	251	<1	1.6	<2	650	0.20
-56 unoxy stg IV anh-gyp dump	< 1	< 1	6	< 2	0.2	33	380	185	244	5	1.2	2	42	3.53
-57 part-oxy stg I vn	< 1	1-10	7	< 2	0.4	24	565	64	224	<1	0.4	<2	39	7.57
-58 oxy talus "bxa" w/ stg I vnlets flt	1-10	1-10	3	< 2	1.5	83	870	75	535	2	1.6	<2	84	0.61

<u>List of Abbreviations</u>

alk trach porph = alkali trachyte porphyry
alt = alteration
anh-gyp = anhydrite-gypsum
bxa = breccia
channel = channel sample
flt = float
jsp = jasperoid (replaced by quartz)
MnOx-FeOx = manganese and iron oxides
mont = montmorillonite
oxy = oxidized
part-oxy = partially oxidized
SAA = same description as above
stage = structural stage
vn = vein
vnlet = veinlet
unoxy = unoxidized
w/ = with

they were collected at the surface from specific alteration zones and mineralized structures. Perhaps most importantly, nearly all samples are overprinted by more than one hydrothermal event (as well as supergene weathering in some cases), rendering them useless for determining geochemical trends within each alteration type.

Fluid Inclusions

Primary and pseudosecondary fluid inclusions are commonly found throughout most of the minerals formed during the three mineralization stages. They are, however, best developed in the fluorite of stage I veins, the quartz of stage II veins, and the anhydrite of the stage IV breccia matrix filling. These inclusions have a maximum dimension of less than 10 µm. They approximate negative crystal forms. Fluid inclusions within the fluorite and quartz are generally liquid-dominated and contain variable liquid to vapor ratios; those within fluorite contain between 1 and 50 volume percent vapor and those within quartz, between 5 and 50 volume percent vapor. Most inclusions within anhydrite are entirely constituted by vapor, although two were found to be liquid dominated. No daughter products or double meniscuses were observed in any of the inclusions.

A crushing study was conducted to determine whether or not the fluid inclusions are overpressured. Polished plates of each sample were immersed in mineral oil at room temperature and then crushed using a dental tool while viewed through a petrographic microscope. Fluorite and quartz fluid inclusions were both found to be overpressured, and the latter consistently yielded larger and more abundant vapor bubbles than the former. Fluid inclusions in the anhydrite yielded no vapor bubbles upon crushing.

Fluid inclusion homogenization temperatures were recorded for the same three minerals in order to infer fluid temperatures of their respective mineralization stages. However, only preliminary data could be obtained due to the small size of the fluid inclusions, their frequent decrepitation upon heating, and previous fluid leakage. Heating studies were conducted using a Roman-Science heating-freezing stage mounted on a Leitz Ortholux II Pol-Bk binocular microscope. Five fluid inclusions within fluorite were tested three times each. All homogenized to liquid at temperatures ranging from 371°C to 425°C, indicating that the stage I fluid was boiling upon formation of the inclusions and that the true trapping temperatures (Roedder, 1981) was probably well below 371°C. Seven quartz fluid inclusions, located immediately outside of the explosion texture zone, were tested three times each. Six of these homogenized to liquid between 198.6°C and 210.6° (avg 203.5°C), while the seventh homogenized at 331.2°C. Apparently the stage II fluids boiled weakly, or effervesced, and the true trapping temperature occurred at, or slightly below, 198.6°C. The vapor-dominated inclusions in the anhydrite neither homogenized nor decrepitated upon heating, and the two containing visible liquid phases homogenized to liquid at temperatures below that required to form anhydrite. It was concluded that these fluid inclusions had leaked previously, perhaps in response to the same stresses which created the curved anhydrite cleavage and crystal faces (Fig. 18). The two containing liquid may have been partially filled at a later time by other fluids. No fluid temperatures can be estimated for the mineralization associated with the stage IV breccia matrix filling.

CHAPTER 9

DISCUSSION OF THE GLOBE HILL DEPOSIT

Structure

Four major structural events occurred at the deposit. Stage I, III, and IV structures are the products of hydrothermal brecciation which developed along pre-existing joints, faults, and fault intersections, while the stage II event produced a system of tectonic structures (Fig. 5).

Each hydrothermal brecciation event produced a distinctive breccia body shape. Breccia of stage I formed in upward-flaring columns which taper to veins at depth (Fig. 5). Stage III breccia formed in at least one vertical column at a pre-existing major fault intersection. Stage IV breccia formed in a vertical, round-topped column (Fig. 5) with small, dike- and column-like apophyses which radiate outward along pre-existing tectonic structures.

Breccia bodies of all three events exhibit textural zonation. Those of stages I and IV grade laterally outward from matrix-supported breccia through fragment-supported breccia to crackle-dominated margins. While the stage IV breccia body grades vertically upward in a similar manner, the stage I breccia bodies grade upward from a vein into a crackle- and breccia-dominated core (Fig. 5). Textural variations within the stage III hydrothermal breccia body consists of alternating fragment-rich and fragment-poor bandings, but more data are needed to extrapolate a zonation pattern for the entire body.

Fluidization, the process of transporting solids in a fluid medium, is evident in all three stages of hydrothermal brecciation. It is indicated in each stage by high I:F ratios and by the mixing of angular and well-rounded heterolithic fragments containing anomalous alteration assemblages. The banded texture of stage III breccia also supports fluidization.

A small amount of fault-induced breccia formed concurrently with stage II tectonic structures. The stage II event generated faults, fault zones, and shear zones, most of which are steeply dipping and strike nearly north-south. Relative displacement along the structures is unclear. Although most display nearly vertical slickensides, some, including the major N-S shear zone (Fig. 5), contain horizontal slickensides. Some of the structures host small, tabular- to lense-shaped breccia bodies along shear zones and column-shaped breccia bodies at structural intersections. These gouge-filled breccias are fault-induced and lack any evidence of hydrothermal activity.

Hydrothermal Fluid Chemistry

The chemistries of the hydrothermal fluids associated with each structural event at the Globe Hill deposit are similar in several ways. They can be qualitatively estimated based on mineral products and their stability parameters, minor and trace elements, fluid inclusion data, extent of alteration zones, and possible mechanisms capable of inducing precipitation.

Fluids Along Stage I Structures - The chemistries of the hydrothermal fluids associated with stage I breccias are inferred from the mineralization and alteration assemblages the fluids produced (Table 1). These assemblages suggest the fluids to have been weakly to moderately alkaline (Stringham, 1952), moderately oxidized, and of low sulfur fugacity (producing minor amounts of sulfides). The fluids must have contained appreciable amounts of Ca, Sr, phosphate, sulfate, and dissolved gases including CO_2 and H_2S in order to form the observed minerals. Resultant zonal wall-rock alteration (Fig. 5) suggests incipient, or weak, hydrogen metasomatism (Hemley and Jones, 1964).

Mixing of hydrothermal fluids with groundwater was possible in this case as evidenced by the restricted extent of sericite-dominated alteration surrounding the breccias and by the absence of advanced hydrolitic alteration (i.e., advanced argillic alteration; Hemley and Jones, 1964). Cooling, redox reactions, and pH changes (buffering) can result from such mixing (Drummond, 1981) and could rapidly equilibrate the two fluids.

Boiling is a possible mechanism capable of promoting mineral precipitation from the fluids along the stage I structures. Evidence that the fluids were boiling includes the development of hydrothermal breccias along the veins, explosion textures in vein quartz, and highly variable vein fluid-inclusion homogenization temperatures and liquid to vapor ratios (Roedder, 1981). Quartz explosion textures indicate that most minerals precipitated immediately after an intense boiling episode. Since boiling causes loss of CO_2 and increased pH of the liquid (Drummond, 1981), precipitation of carbonate and celestite is then promoted (Holland and Malinin, 1979). The decrease in temperature and pressure of a boiling liquid encourages precipitation of quartz and fluorite (Holland and Malinin, 1979). The deposition of sulfates, oxides, and phosphates may be induced by the oxidation of the boiling liquid (Drummond, 1981). Sulfide formation may not be directly facilitated by boiling, as incomplete oxidation of H_2S in the liquid often permits sulfide precipitation upon lowering temperature and pressure (Barnes, 1979).

Fluids Along Stage II Structures - Fluid chemistries along the vein-filled stage II tectonic structures are inferred from the mineralization and alteration assemblages which were produced by them (Table 1). Stage II fluids were moderately alkaline (Stringham, 1952), moderately oxidized, of low sulfur fugacity, and must have contained appreciable amounts of Sr and dissolved gases including CO_2 and H_2S. The resultant wallrock alteration suggests intermediate hydrogen metasomatism to have occurred (Hemley and Jones, 1964). As with the stage I fluids, mixing with groundwater is suggested by the restricted extent of the wallrock alteration and by the lack of advanced hydrolitic alteration.

Boiling may have led to mineral precipitation along the stage II vein structures. Evidence includes the occurrence of adularia in the vein assemblage (Hemley and Jones, 1964; Ellis, 1979), explosion texture in vein quartz, and the variable vein fluid-inclusion homogenization temperatures and liquid to vapor ratios. The presence of most vein minerals within the explosion texture zone indicates their coprecipitation with quartz during an intense boiling episode. The specific causes of mineral precipitation from these boiling fluids are the same as those discussed above for stage I fluids. Additionally, although boiling was indeed intense in this case, exsolved gases must have escaped unimpeded to the surface since no hydrothermal breccia developed.

The fluids along the gangue-free stage II tectonic structures are inferred from the resultant alteration and disseminated mineralization (Table 1) to have been moderately alkaline (Stringham, 1952), weakly oxidized, and of moderate sulfur fugacity. Wallrock alteration (Fig. 5) also suggests intermediate hydrogen metasomatism to have occurred (Hemley and Jones, 1964).

Metasomatic interactions of the fluids with wallrock minerals, accompanied by mixing with groundwater, probably produced the alteration and mineralization along gangue-free structures. The relatively widespread extent of alteration and dissemination suggests metasomatic interactions of fluids with wallrock minerals to be the main precipitation mechanism. Cation exchange, redox reactions, and pH changes are all possible methods for gradual equilibration of fluids to wallrock. No evidence was found to support boiling as a precipitation mechanism, but mixing of fluids with groundwater could have prompted minor precipitation.

Fluids Along Stage III Structures - The hydrothermal fluid associated with the stage III intrusive breccia is inferred from the resultant matrix alteration assemblage (Table 1) to have been weakly to moderately alkaline (Stringham, 1952), strongly oxidized, and of very low sulfur fugacity. Incipient to weak, but thorough, hydrogen metasomatism (Hemley and Jones, 1964) is also suggested.

Metasomatic interaction of fluid with the fine-grained, permeable matrix material, and to a lesser extent with the large breccia fragments and surrounding wallrock, probably created the stage III alteration assemblage. Complete alteration of the matrix and partial alteration of the fragments and wallrock signify rapid equilibration of fluid with the matrix.

Fluids Along Stage IV Structures - Hydrothermal fluids associated with the stage IV central core zone are deduced from mineralization and alteration assemblages (Table 1) to have been moderately alkaline (Stringham, 1952), moderately oxidized, and of moderate sulfur fugacity. They must have contained abundant Ca, Sr, sulfate, and dissolved gases including CO_2 and H_2S in order to form the observed minerals. Breccia fragment alteration (Fig. 5) also suggests intermediate hydrogen metasomatism to have occurred (Hemley and Jones, 1964).

Boiling is a possible precipitation mechanism for the central core zone fluids. Evidence for boiling includes the presence of hydrothermal breccia and of crude explosion textures in celestite. Both celestite and anhydrite have retrograde solubilities in aqueous solutions at temperatures roughly less than 350°C (Holland and Malinin, 1979) which prohibit their precipitation upon cooling. Boiling, however, would saturate the liquid with respect to both minerals and lower pressures, facilitating their precipitation. The influence of boiling upon precipitation of the remaining assemblage minerals is similar to that discussed in the section of fluids in stage I structures.

The mineralization and alteration assemblages associated with the stage IV peripheral breccia zone reflect the chemistry of the hydrothermal fluids which produced them (Table 1). The assemblages suggest the fluids to be moderately alkaline (Stringham, 1952), strongly oxidized, and of very low sulfur fugacity. The breccia-fragment and wallrock alteration assemblage (Fig. 5) is suggestive of weak hydrogen metasomatism (Hemley and Jones, 1964).

Boiling, metasomatic wallrock and breccia-fragment interactions, and groundwater mixing are all possible precipitation mechanisms for the stage IV peripheral zone fluids. Boiling is suggested by the extensively-developed hydrothermal breccia of this zone. However, assuming that the fluids present are the exsolved, vapor-dominated components of the central core zone liquid, this is probably not an important mechanism. Moderate wallrock and fragment alteration support metasomatism and groundwater mixing as the two major precipitation mechanisms. These mechanisms could effectively promote fluid-wallrock and fluid-groundwater equilibration, terminating further alteration. Fluid-groundwater mixing would also cool the fluid, condense the steam (the condensable component of the fluid), terminate breccia development, and promote mineral precipitation from the fluid's liquid component.

Summary - Mineralization and alteration assemblages associated with each structural event at Globe Hill have been used to infer the chemistries of their parent fluids. The assemblages suggest weakly to moderately alkaline and moderately oxidized fluids with relatively low sulfur fugacities. Some fluids along stage I, II, and IV structures must have contained appreciable amounts of Ca, Sr, and dissolved gases including CO_2 and H_2S in order to form the observed minerals. Zonal wallrock alteration assemblages indicate intermediate to weak metasomatic reactions adjacent to each structure.

Boiling of the hydrothermal fluids may have led to precipitation of nearly all open-space mineral assemblages observed. Evidence for boiling fluids includes the development of hydrothermal breccias, often along veins; explosion textures in vein quartz and celestite; the occurrence of adularia in some vein assemblages; and highly-variable vein fluid-inclusion homogenization temperatures and liquid to vapor ratios. Boiling of a hydrothermal liquid causes loss of CO_2 and other dissolved gases, increased pH of the liquid, decreased temperature and pressure of the liquid, concentration of non-volatile components in the liquid, and oxidation of components in the liquid. These changes in fluid chemistry probably promoted precipitation of the minerals observed in each of the structural stages.

Metasomatic wallrock interactions and mixing of hydrothermal fluids with groundwater are possible precipitation mechanisms for each fluid. These mechanisms may have been primarily responsible for the formation of disseminated mineralization and alteration along stage II tectonic structures and in the stage IV hydrothermal breccia peripheral zone. Cation exchange, redox reactions, and pH changes accompanied cooling, which tend to equilibrate the fluids with altered wallrock material, and terminated further alteration. Differing rates of metasomatic wallrock reactions and groundwater mixing for each event may account for variations in their extent, type, and degree of surrounding alteration.

Comparison With Other Deposits at Cripple Creek

Mineralization and alteration assemblages associated with stage I and II structures at the Globe Hill deposit are similar to those of the El Paso and Ajax vein systems (Fig. 2) described in chapter 3. This implies that the Globe Hill fluids may have been chemically similar to the dilute, late-stage, low-temperature fluids which deposited tellurides at the two vein-type deposits. Unlike the Globe Hill system, however, neither the Ajax nor the El Paso systems produced appreciable amounts of hypogene sulfates, oxides, or phosphates, and wallrock alteration is extremely restricted. Cooling of hydrothermal fluids are reported to be the major precipitation mechanism in both vein systems. No evidence for boiling has been found at the El Paso, and only minor boiling occurred at the Ajax. This is in strong contrast to Globe Hill, where boiling was so intense that it created many of the structures and caused mineral precipitation at the same time.

An interesting comparison can be made between the high-grade mineralization at the Cresson mine (Fig. 2; Patton and Wolf, 1915) and the very low-grade mineralization associated with the stage IV hydrothermal breccia body at Globe Hill. As mentioned in chapter 3, the Cresson mine is developed in a basaltic diatreme which cuts the Cripple Creek Breccia (Thompson et al., in press). Much of the ore produced has been low grade and found as disseminations in irregular shoots (Loughlin and Koschmann, 1935) within the diatreme structure. A few large vugs were discovered, one of which was lined with a six-inch thick, porous material assaying 500 to 800 oz/t gold (Patton and Wolf, 1915) and containing celestite needles, a white, earthy material (possibly montmorillonite), calaverite blades, chalcedony, etched quartz crystals, pyrite, and dolomite rhombs (some psuedomorphically replaced by quartz). Celestite and calaverite were reportedly intergrown in a manner suggesting coprecipitation. The surrounding wallrock was moderately silicified (by replacement), a feature uncommon district-wide. Abundant celestite, montmorillonite, and anomalous silicified wallrock fragments in the stage IV Globe Hill hydrothermal breccia body suggests that similar processes may have formed the two deposits. Perhaps the similarities are due to hydrothermal leaching of basaltic material at depth, which could supply the large amount of Ca and Sr necessary to form the unique mineralogy of the Globe Hill deposit. To date, however, little direct evidence for the occurrence of basaltic rocks has been found at Globe Hill. A single fragment which is possibly basalt was observed within the alkali trachyte porphyry, and one fragment of possible gabbroic composition was found within the stage III intrusive breccia.

CHAPTER 10

ORIGIN OF THE DEPOSIT

The Globe Hill deposit is epithermal, polymetallic, and structurally controlled. The development of episodic and overlapping structures, mineralization, and alteration post-date the relatively shallow emplacement and crystallization of a pyroxene-bearing alkali trachyte porphyry within the Cripple Creek Breccia (Fig. 5). Associated hydrothermal fluids are inferred to have been composed of meteoric water; were weakly to moderately alkaline, moderately oxidized, and of relatively low sulfur fugacity; and contained appreciable amounts of Ca, Sr and dissolved gases. These solutions were probably convectively driven by the thermal gradient generated by a heat source at depth. The presence of calcium, strontium, and the thermal anomaly may be related to the late alkali basalt igneous activity of the entire district. In genetic terms, the hot-springs depositional model proposed by Berger and Eimon (1982) is very similar to the processes envisioned by this author to have created the Globe Hill deposit.

The stage I hydrothermal breccia bodies formed along pre-existing planar structures which cut the relatively-impermeable alkali trachyte porphyry. Weakly to moderately alkaline hydrothermal fluids were confined to faults until boiling was initiated, possibly by a sudden pressure drop during tectonic readjustments. Exsolved vapor then hydrofractured and brecciated the alkali trachyte porphyry in an upward-flaring zone. Boiling liquid either accompanied or immediately followed the escaping vapor and precipitated minerals in the open-space breccia matrix. Fluid pressures were high along the feeder structures and in the center of each breccia body. This created the matrix-supported texture and caused the upward fluidized transport of well-rounded, anomalous wallrock fragments. The exsolved vapors may have escaped to the atmosphere, but were more likely buffered by groundwater and wallrock interactions.

The earliest stage II tectonic activity created irregular shear zones with dilated, or pinch and swell shaped, permeable zones which cut the relatively-impermeable subvolcanic mass. These structures were filled with a moderately alkaline, boiling solution which precipitated minerals but did not create hydrofracturing. The relatively-restricted wallrock alteration represents intermediate hydrogen metasomatism, suggesting that the vein fluids were buffered by groundwater and wallrock interactions.

The later stage II tectonic activity produced large, steep, planar faults and shear zones which cut the relatively impermeable host rock. Weakly to moderately alkaline fluids passed through the structures and permeated the adjacent wallrock. The resultant wallrock mineralization and alteration represents intermediate hydrogen metasomatism caused by solutions which did not boil.

The stage III intrusive breccia is unusual for the Globe Hill deposit. It has intruded the largest and deepest stage II structure (the N-S shear zone) at the intersection of several major faults. The breccia body was altered by a moderately-alkaline, strongly-oxidized hydrothermal fluid which did not appreciably affect the stage II sericitic-altered shear zone within which it occurs. This suggests that the same breccia-forming fluid is responsible for the stage III alteration. The geometry and texture of the breccia are indicative of vapor-dominated fluidization, which may have resulted from a phreatic or phreatomagmatic explosion as groundwater at depth in the N-S shear zone was flashed to steam by magma invading upward along the structure.

The stage IV hydrothermal breccia was created when moderately-alkaline, boiling fluids formed an extensively-hydrofractured body and transported wallrock fragments into it from depth. The anhydrite-cemented central core zone of this body appears to have formed around upward-propagating, fragment-free columns of anhydrite. It is presumed that boiling, hydrothermal brecciation, and sulfate precipitation occurred concommitantly in this zone. The manner in which voluminous amounts of montmorillonite formed as veins and as peripheral zone breccia matrix is unclear, although it may be related to the processes which silicified heterolithic fragments found in the central core zone. The extent and degree of stage II alteration suggests that groundwater and fragment/wallrock interactions in the peripheral zone may have strongly buffered the hydrothermal fluids.

It is possible that all episodes of hydrothermal fluids responsible for producing the Globe Hill deposit were initially composed of nearly neutral to weakly-alkaline, meteoric water with low oxygen fugacity. Near-surface episodic boiling, triggered by tectonic readjustments along pre-existing structures, created hydrofracturing, brecciation, and upward fluidized transport of wallrock material. Boiling might also have increased the pH and oxygen fugacity, facilitating the formation of moderately-alkaline and oxidized mineral assemblages. Comparisons with deeper vein deposits in the district tentatively reveal the mineralized structures at Globe Hill to be the high-level, near-surface portion of a deep vein system. Anomalous breccia fragments in the stage I and III structures contain abundant, fracture-controlled, secondary potash-feldspar, a common feature in the deep, high-grade precious-metal vein deposits at Cripple Creek (Lane, 1976; Dwelley, 1984) and elsewhere (Buchanan, 1981). An alkali basalt igneous body at depth may have generated the thermal gradient required to convect the Globe Hill fluids. It also may have supplied the Ca and Sr (neither of which is a common constituent of the alkali trachyte porphyry host rock) required to produce the observed mineral assemblages.

CHAPTER 11

RECOMMENDATIONS

Future research on the Globe Hill deposit should encompass the following:

1) A study of hypogene and supergene clay mineralogy to detect zonal patterns resulting from each alteration event. Lateral and vertical clay zonation for the separate alteration events, or for the entire deposit, could further refine the proposed genetic model.
2) A thorough trace-element study involving extensive surface and core sampling for analysis of U, Th, and rare earths as well as elements reported in this thesis. These data would refine genetic models of the deposit, and, if combined with district-wide studies such as Gott et al. (1969), could establish geochemical criteria for exploration purposes.
3) A complete fluid inclusion study of each of the three mineralization events. Data should include homogenization and freezing (clathrate, if present) temperatures, and analysis of dissolved gases. This would aid estimation of actual fluid temperatures, salinities, pressures, fO_2, fS_2, pH, metal complexing, and formation depth of the deposit.

4) Whole-rock and density analyses of altered and unaltered alkali trachyte porphyry. This would permit a better understanding of the alteration events in terms of gain/loss relationships.

5) Continuation of thin and polished section studies with the aid of microprobe analyses. The compositional and textural data obtained would further document the paragenesis and fluid evolution within and between hydrothermal events.

6) Isotopic studies involving hydrogen and oxygen analyzed from minerals of each hydrothermal event. These data would suggest relative amounts of meteoric versus magmatic water. Lead isotope data could be used to identify the source of lead, and presumably other metals, with comparison to other rock types in the district.

7) Age dates (K/Ar) on unaltered alkali trachyte porphyry and possibly the sericite or adularia of each hydrothermal event.

8) Geophysical surveys, including gravity, magnetic, and electrical methods (induced polarization, resistivity, and electromagnetics). This would aid in the delineation of unexposed structures, rock types, alteration types, and disseminated sulfides.

9) Detailed study of anomalous fragments in stage I, III, and IV hydrothermal breccias, including lithology, mineralization, alteration, and geochemical trace elements analyses, to determine potential for ore at depth.

10) Mapping and sampling of the deposit operated by Nerco Minerals Company half a kilometer to the southeast, and of the Chicago and Cripple Creek Tunnel beneath the Globe Hill deposit. Comparison of these studies to the information presented in this thesis may provide valuable insight as to the genesis of the near-surface, low-grade, breccia-hosted mineral deposits at Cripple Creek.

11) Shallow core drilling in favorable alteration zones surrounding the Globe Hill pit, and deep core drilling beneath the deposit. This would provide data regarding lithology, structure, mineralization, and alteration of both near-surface geology and the potential for deeper, vein-type deposits.

REFERENCES

Argall, P., 1905, Report on Globe Hill properties to the Stratton-Cripple Creek Mining and Development Company: unpub. report, 49 p.

Argall, P., 1908, Rock oxidation at Cripple Creek: Mining and Scientific Press: Vol. 96, No. 26, p. 883-886.

Barker, F., Wones, D.R., Sharp, W.N., and Desborough, G.A., 1975, The Pikes Peak batholith, Colorado Front Range, and a model for the origin of the gabbro-anorthosite-syenite-potassic granite suite: Precambrian Research, Vol. 2, 97-160.

Barnes, H.L., 1979, Solubilities of ore minerals: in H.L. Barnes (ed.), Geochemistry of hydrothermal ore deposits, 2nd edition, John Wiley and Sons, New York, p. 404-460.

Berger, B.R., and Eimon, P.I., 1982, Comparative models of epithermal silver-gold deposits: Soc. Mining Engineers AIME Preprint 82-13, 14 p.

Buchanan, L.J., 1981, Precious metal deposits associated with volcanic environments in the southwest; in Relations of tectonics to ore deposits in the southern Cordillera, W.R. Dickinson and W.D. Payne (eds.), Arizona Geol. Soc. Digest Vol. 14, p. 237-262.

Chapin, C.E., 1979, Evolution of the Rio Grande rift: A summary, in Rio Grande rift: tectonics and magmatism: R.I. Riecker (ed.), Am. Geophys. Union, Washington, D.C., p. 1-5.

Chapin, C.E., and Epis, R.C., 1964, Some stratigraphic and structural features of the Thirtynine Mile volcanic field, central Colorado: The Mountain Geologist, Vol. 1, p. 145-160.

Cross, W., and Penrose, R.A.F., Jr., 1895, Geology and mining industries of the Cripple Creek district, Colorado: U.S. Geol. Survey 16th Ann. Rept., pt. 2, p. 1-209.

Drummond, S.E., Jr., 1981, Boiling and mixing of hydrothermal fluids: chemical effects on mineral precipitation: unpub. Pennsylvania State Univ. Ph.D. thesis, 380 p.

Dwelley, P.C., 1984, Geology, mineralization, and fluid inclusion analysis of the Ajax vein system, Cripple Creek mining district, Colorado: unpub. Colorado State Univ. M.S. thesis, 167 p.

Ellis, A.J., 1979, Explored geothermal systems: in H.L. Barnes (ed.), Geochemistry of hydrothermal ore deposits, 2nd edition, John Wiley and Sons, Inc., New York, p. 632-683.

Fahley, M.P., 1981, Fluid inclusion study of the Tonopah district, Nevada: unpub. Colorado School of Mines M.S. thesis, 106 p.

Gott, G.B., McCarthy, J.H., Jr., VanSickle, G.H., and McHugh, J.B., 1967, Distribution of gold, tellurium, silver, and mercury in part of the Cripple Creek district, Colorado: U.S. Geol. Survey Circ. 543, 8 p.

Gott, G.B., McCarthy, J.H., Jr., VanSickle, G.H., and McHugh, J.B., 1969, Distribution of gold and other metals in the Cripple Creek district, Colorado: U.S. Geol. Survey Prof. Paper 625-A, p. A1-A17.

Hemley, J.J., and Jones, W.R., 1964, Chemical aspects of hydrothermal alteration with emphasis on hydrogen metasomatism: Economic Geology, Vol. 59, p. 538-569.

Holland, H.D., and Malinin, S.D., 1979, The solubility and occurrence of non-ore minerals: in H.L. Barnes (ed.), Geochemistry of hydrothermal ore deposits, 2nd edition, John Wiley and Sons, Inc., New York, p. 461-508.

Hutchison, C.S., 1974, Laboratory handbook of petrographic techniques: John Wiley and Sons, Inc., New York, 527 p.

Hutchinson, R.M., and Hedge, C.E., 1968, Depth-zone emplacement and geochronology of Precambrian plutons, central Colorado Front Range, in Abstracts for 1967: Geol. Soc. Amer. Spec. Paper 115, p. 424-425.

Keener, J.H., 1962, The Stratton Cripple Creek Mining and Development Company, Cripple Creek, Colo.: unpub. report, 21 p.

Kleinkopf, M.D., Peterson, D.L., and Gott, G., 1970, Geophysical studies of the Cripple Creek mining district, Colorado: Geophysics, Vol. 35, No. 3, p. 490-500.

Koschmann, A.H., 1941, New light on the geology of the Cripple Creek district and its practical significance: Colorado Mining Assoc., Denver, Colorado, January, 1941, p. 3-28.

Koschmann, A.H., 1949, Structural control of the gold deposits of the Cripple Creek district, Teller County, Colorado: U.S. Geol. Survey Bull. 955-B, p. 19-60.

Koschmann, A.H., 1960, Cripple Creek district, in Guide to the geology of Colorado: R.J. Weimer, and J.D. Haun (eds.), p. 185-187.

Koschmann, A.H., and Loughlin, G.F., 1965, Mine maps of the Cripple Creek district, Colorado: U.S. Geol. Survey Open-file rept. #65-90, 18 portfolios (528 maps) and index.

Lane, C.A., 1976, Geology, mineralogy, and fluid inclusion geothermometry of the El Paso gold mine, Cripple Creek, Colorado: unpub. Univ. of Missouri-Rolla M.S. thesis, 103 p.

Lewis, A., 1982, Producing gold for $160/Tr Oz in Victor, Colorado: Engr. Min. Journal, Vol. 183, No. 10, p. 102-107.

Lindgren, W., and Ransome, F.L., 1906, Geology and gold deposits of the Cripple Creek district, Colorado: U.S. Geol. Survey Prof. Paper 54, 516 p.

Lipman, P.W., 1969, Alkalic and tholeiitic basaltic volcanism and development of the Rio Grande depression, southern Colorado and northern New Mexico: Geol. Soc. Am. Bull. 80, p. 1343-1354.

Lipman, P.W., 1983, Tectonic setting of the mid to late Tertiary in the Rocky Mountains - a review, in The genesis of Rocky Mountain ore deposits: changes with time and tectonics: Denver Region Exploration Geologists Society Symposium, Nov. 4-5, 1982, Denver, Colorado, p. 128-131.

Lipman, P.W., Prostka, H.J., and Christiansen, R.L., 1972, Cenozoic volcanism and plate tectonic evolution of the western United States: Pt. I; Early and middle Cenozoic, in A discussion on volcanism and the structure of the Earth: Royal Soc. London Philos. Trans., ser. A, Vol. 271, p. 217-248.

Lipman, P.W., and Mehnert, H.H., 1975, Late Cenozoic basaltic volcanism and development of the Rio Grande depression in the southern Rocky Mountains, in Cenozoic history of the southern Rocky Mountains: B.F. Curtis (ed.), Geol. Soc. Amer. Memoir 144, p. 119-154.

Loughlin, G.F., and Koschmann, A.H., 1935, Geology and ore deposits of the Cripple Creek district, Colorado: Colo. Sci. Soc. Proc., Vol. 13, No. 6, p. 217-435.

Marvin, R.F., Young, E.J., Mehnert, H.H., and Naeser, C.W., 1974, Summary of radiometric age determinations on Mesozoic and Cenozoic igneous rocks and uranium and base metal deposits in Colorado: Isochron/West, no. 11, 41 p.

McDowell, F.W., 1971, K-Ar ages of igneous rocks from the western United States: Isochron/West, no. 2, p. 1-16.

Patton, H.B., and Wolf, H.J., 1915, Preliminary report on the Cresson gold strike at Cripple Creek, Colorado: Colorado School of Mines Quarterly, Vol. 9, No. 4, p. 3-15.

Peters, S.G., 1982, Evaluation of Gold Resources, Inc. property, 1981-1982, Cripple Creek district, Colorado: unpub. report, 181 p.

Roedder, E., 1981, Origin of fluid inclusions and changes that occur after trapping: in L.S. Hollister and M.L. Crawford (eds.), Fluid inclusions: applications to petrology, Mineralogical Assoc. of Canada, Short course handbook, Vol. 6, p. 101-137.

Sillitoe, R.H., and Bonham, H.F., Jr., 1984, Volcanic land forms and ore deposits: Economic Geology, Vol. 79, p. 1286-1298.

Sinclair, A.J., 1974, Selection of threshold values in geochemical data using probability graphs: Jour. of Geochemical Exploration, Vol. 3, p. 129-149.

Sprague, M., 1953, Money Mountain: Univ. of Nebraska Press, Lincoln, Nebraska, 342 p.

Steven, T.A., 1975, Middle Tertiary volcanic field in the southern Rocky Mountains, in Cenozoic history of the southern Rocky Mountains: B.F. Curtis (ed.), Geol. Soc. Am. Memoir 144, p. 75-94.

Stringham, B., 1952, Fields of formation of some common hydrothermal-alteration minerals: Economic Geology, Vol. 47, p. 661-664.

Thompson, T.B., Trippel, A.D., and Dwelley, P.C., in press, Mineralized veins and breccias of the Cripple Creek district, Colorado: Economic Geology.

Tweto, O., 1975, Laramide orogeny in the southern Rocky Mountains, in Cenozoic history of the southern Rocky Mountains: B.F. Curtis (ed.), Geol. Soc. Am. Memoir 144, p. 1-44.

Tweto, O., 1979, The Rio Grande rift system in Colorado, in Rio Grande rift: tectonics and magmatism: R.I. Riecker (ed.), Am. Geophys. Union, Washington, D.C., p. 33-56.

Wobus, R.C., Epis, R.C., and Scott, G.R., 1976, Reconnaissance geologic map of the Cripple Creek-Pikes Peak area, Teller, Fremont, and El Paso Counties, Colorado: U.S. Geol. Survey Map MF-805.

Woolsey, T.S., McCallum, M.E., and Schumm, S.A., 1975, Modeling of diatreme emplacement by fluidization: Physics and Chemistry of the Earth, Vol. 9, Pergamon Press, New York, p. 29-42.

Plate I

Geologic map of area surrounding Globe Hill, Cripple Creek district, Colorado

contact

surface projection of the Chicago and Cripple Creek Tunnel

zone of abundant hydrothermal breccia bodies

shaft

adit

open pit

road

building

N

Tertiary — undifferentiated Cripple Creek Breccia and alkaline igneous rock

Precambrian — granodiorite

biotite gneiss — muscovite schist

contour interval 5 ft. (1.5 m)

scale 1:6000

200 0 200 meters

500 0 500 feet

ADT 1985

Plate 2
Geologic outcrop map of the Globe Hill pit
Cripple Creek district, Colorado
GLOBE HILL
(elev. 3183m)
Summit
Deerhorn
DDH-450SE
S53E -45°
450 ft.
137 m
DDH-500SE
S42E -45°
511 ft.
156 m
DDH-150SE
S49E -46°
481 ft.
146 m
DDH-200NW
N46W -47°
471 ft.
144 m
DDH-100NW
N40W -55°
500 ft.
152 m
DDH-150NW
N43W -47°
487 ft.
148 m
DDH-000NW
N41W -49°
409 ft.
125 m
EXPLANATION
note: entire map area is pyroxene-bearing alkali trachyte porphyry
outcrop
alkali trachyte dike
fault (dashed where approximate, dotted where inferred)
shear zone (dotted where inferred)
tectonic breccia (fault-induced)
hydrothermal breccia
hydrothermal crackle
vein (dotted where inferred)
rock sample location (random chip and channel samples)
shaft
number
bearing angle
depth
diamond drill hole location (arrow indicates bearing)
boundary of area mapped
chalcedony-celestite-pyrite (fracture, vein, and matrix filling)
sericite-chlorite-carbonate-montmorillonite-pyrite (alteration)
chlorite-sericite-pyrite-quartz (alteration)
sericite-montmorillonite-carbonate-pyrite (alteration)
N
contour interval = 2 ft. (0.61m)
scale 1:480
100 0 100
feet
10 0 10
meters
ADT 1985